AN ABSTRACT OF THE THESIS OF

Gerald Lum Sing (Name) for the degree Master of Science (Degree)

in Civil Engineering (Department) presented on March 29, 1976 (Date)

Title: COMPUTER MODEL: MASS TRANSFER FROM SINGLE RISING GAS BUBBLES IN WATER

Abstract approved: Redacted for Privacy

Mass transfer from single rising gas bubbles is generally studied by taking motion pictures of the rising bubbles and analyzing the film for the instantaneous mass transfer coefficient. In this study, a different approach was taken for the analysis of mass transfer. This analysis solved the simultaneous differential equations describing mass transfer by numerical techniques. The computer model developed is restricted to pure single gas bubbles in water, with diameters in the size range $0.01 \leq$ diameter ≤ 0.30 cm. Given a bubble's initial diameter and height of water over the bubble, the model predicts the bubble's position and moles of gas present in the bubble at any other time.

The bubble rise velocity was calculated by considering a force balance on a spherical bubble and used theoretical values of drag coefficients based on a sphere. Correlations presented by Hamerton and Garner, Frossling, and Weiner were used to solve for K_L, the convective mass transfer coefficient.

The time dependent behavior of K_L, attributed to the accumulation of surface active agents at the rising bubble's interface, was

accounted for by the development of a bubble age parameter, termed critical time.

The differential equations were solved by a Runge-Kutta-Merson routine, and the model applied to a carbon dioxide-water system. The results were compared to data collected in the investigations of Deindoerfer, Garbarini, and Datta. The computer predictions, with the inclusion of the critical time parameter, corresponded closely to data presented by the three investigators. The model, without the critical time parameter, predicted mass transfer rates much higher than those presented in the three investigations.

The model was extended to pure oxygen-water and air-water systems to aid in the modeling of gas dispersion equipment used in aeration ponds. Predictions indicate that the initial bubble diameter has a significant role on the overall mass transfer.

Computer Model: Mass Transfer from Single Rising Gas Bubbles in Water

by

Gerald Lum Sing

A THESIS

submitted to

Oregon State University

in partial fulfillment of
the requirements for the
degree of

Master of Science

June 1976

APPROVED:

Redacted for Privacy

Professor of Chemical Engineering in charge of major

Redacted for Privacy

Head of Department of Civil Engineering

Redacted for Privacy

Dean of Graduate School

Date thesis is presented MARCH 29, 1976

ACKNOWLEDGMENT

The author wishes to express his deepest appreciation to:

Dr. Charles E. Wicks for his endless enthusiasm, encouragement, inspiration, and advice.

The Civil and Chemical Engineering Departments for financial assistance received, without which this work would have not been possible.

The Chemical Engineering secretaries who so graciously typed and corrected this work.

The Chemical Engineering graduate students who knowingly and unknowingly contributed ideas incorporated into this work.

TABLE OF CONTENTS

LIST OF ILLUSTRATIONS

APPENDICES

COMPUTER MODEL: MASS TRANSFER FROM SINGLE RISING GAS BUBBLES IN WATER

I. INTRODUCTION

Previous research and experimentation in gas absorption has often centered on the study of single bubbles rising through liquids. The behavior of single bubbles is studied to determine the fundamental mechanisms involved in the absorption of gases. The experimental technique of limiting study to single bubbles permits an analysis simplified to a few specific variables.

Analysis usually begins by describing mass transfer from the bubble with appropriate differential equations. Assumptions are then introduced into the differential equations, converting them to a form that can be solved by photographic techniques. Motion pictures are taken of a bubble's ascent and the film is then analyzed. This analysis generates finite difference terms which are used in the solution of the converted equations to determine instantaneous mass transfer rates. The drawback of the photographic method is that bubble history and instantaneous mass transfer rates must be determined by setting up laboratory equipment, taking motion pictures, and analyzing the film. This method also has image resolution limitations which restricts its application to certain gas-liquid systems.

The presence of surface active agents (surfactants) is known to retard mass transfer from bubbles and contribute to scattering of data in gas absorption experiments. The effects of these agents have not been satisfactorily incorporated into mass transfer theory, and great care is usually taken to eliminate them from research

experiments. In contrast, industrial processes will invariably contain trace amounts of surface active agents that will inhibit mass transfer. As a result, experiments in gas absorption may not be including an important factor of mass transfer which occurs in real processes.

Modeling and design of gas dispersion equipment in aeration ponds usually involves empirical correlations based upon several equipment variables. The variables used include gas flow rate, type of sparger, sparger orientation, and depth of sparger. [4] Use of these parameters in correlations reflects the lack of understanding of the fundamental mass transfer mechanisms.

The intent of this study is to model rising gas bubbles by solving the same differential equations using numerical techniques. This has the advantage of studying single bubble behavior without taking experimental data, and is capable of modeling some gas-water systems otherwise awkward for experimental setup. The carbon dioxide-water system will be modeled and the results compared to data collected in other investigations. The model will then be extended to include pure oxygen-water and air-water systems.

II. THEORETICAL CONSIDERATIONS

When a gas bubble has a slight solubility in a liquid, the mass transfer from the rising bubble is limited by the resistance in the liquid film surrounding the bubble. A material balance, accounting for the moles of gas present in the bubble at any time may be written as a differential equation:

$$\frac{dn}{dt} = -K_L a \, (C_{AS} - C_{A\infty}) \qquad (1)$$

where n is the moles of gas, t is time, K_L, is the convective mass transfer coefficient, a is the area through which mass transfer occurs (bubble surface area), C_{AS} is the concentration of gas in the liquid which is related by equilibrium relations to the composition of the gas in the bubble, and $C_{A\infty}$ is the concentration of gas in the bulk liquid. The negative sign on equation (1) implies that gas is transferred from the bubble to the liquid; accordingly, the amount of gas within the bubble will always decrease.

The instantaneous velocity of the bubble is written as:

$$\frac{dz}{dt} = -V_o \qquad (2)$$

where V_o is the bubble's rise velocity, and z is the bubble's position.

Equation (1) may be simplified if the following assumptions are made:

1. The gas is pure
2. The gas is ideal
3. Henry's law applies. (Appendix) [11]

4. The bulk concentration of gas, $C_{A\infty}$ is essentially zero.

5. The system is isothermal.

6. Humidification and counterdiffusion effects are negligible.

7. Surface tension effects are negligible. (Appendix)

By the ideal gas law, the moles of gas present are related to the bubble's pressure, P, temperature, T, and volume, V, by:

$$n = \frac{PV}{RT} \tag{3}$$

where R is the ideal gas constant. The time derivative of equation (3) under isothermal conditions is:

$$\frac{dn}{dt} = \frac{1}{RT}\left(\frac{PdV}{dt} + \frac{VdP}{dt}\right) \tag{4}$$

The assumption that the gas is pure implies that only one component material balance equation is required to describe the mass transfer from the bubble. For a mixture of gases separate differential equations must be written to describe mass transfer for each component, and a system of differential equations must be solved for the total moles of gas present. Negligible humidification and counterdiffusion effects implies that counterdiffusion of liquid vapor and dissolved gases into the bubble is negligible and will not add to the moles of gas present in the bubble. Accounting for these effects would also generate other differential equations, resulting in a system of equations to be solved simultaneously.

The pressure within a bubble varies with the depth of liquid and bubble size. Where surface tension effects are negligible, the bubble's internal pressure is described by the expression:

$$P = P_{ATM} + \rho_L g z \tag{5}$$

where P_{ATM} is the atmospheric pressure, ρ_L, is the liquid density, g is the gravitational constant, and z is the height of liquid over the bubble. In the case of an incompressible liquid, the time derivative of equation (5) is:

$$\frac{dP}{dt} = \rho_L g \frac{dz}{dt} \tag{6}$$

Henry's law applies for systems where the concentration of gas in the liquid is small. Henry's law is written as:

$$x = HP_i = \text{mole fraction of gas} \tag{7}$$

where H, is the Henry's law constant, there are different Henry's law constants for each gas-water system. P_i is the partial pressure of the gas, and x is the mole fraction of gas in the liquid. The mole fraction of gas may be written as:

$$\text{mole fraction gas} = \frac{\text{moles gas/cm}^3}{\text{moles gas/cm}^3 + \text{moles liquid/cm}^3}$$

But the moles gas/cm^3 is equal to C_{AS}, the concentration of gas in the liquid, and the moles liquid/cm^3 is equal to ρ_L/molecular weight of liquid. For water, ρ_L is 0.995 g/cm^3 @ 298°K and the molecular weight of water is 18 g/g mole; accordingly, the moles of liquid/cm^3 is 0.055278. Upon substitution of C_{AS} for moles gas/cm^3 in equation (7) yields:

$$\frac{C_{AS}}{C_{AS} + 0.055278} = HP_i$$

Solving for C_{AS} one obtains:

$$C_{AS} = \frac{HP_i \cdot 0.055278}{1 - HP_i}$$

and when the constant 0.055278 is designated PRO, C_{AS} becomes

$$C_{AS} = \frac{HP_i \cdot PRO}{1 - HP_i} \tag{8}$$

Equation (1) may be rearranged to yield:

$$K_L = - \frac{dn/dt}{a(C_{AS} - 0)}$$

If equation (4) is substituted for dn/dt, the following equation results:

$$K_L = - \frac{\frac{1}{RT}\left(\frac{PdV}{dt} + \frac{VdP}{dt}\right)}{a(C_{AS})}$$

Further simplification is obtained if equation (8) is substituted for C_{AS}:

$$K_L = - \frac{(1 - HP_i)}{RTa\ HP_i \cdot PRO}\left(\frac{PdV}{dt} + \frac{VdP}{dt}\right)$$

Finally, with substitution of equation (6) for dP/dt one obtains:

$$K_L = - \frac{(1 - HP_i)}{RTa\ HP_i \cdot PRO}\left[\frac{PdV}{dt} + V\rho_L g \frac{dz}{dt}\right] \tag{9}$$

The evaluation of K_L by the photographic method requires the solution of equation (9) which, in turn, requires the time derivatives

dV/dt and dz/dt. Motion pictures of the rising bubble are taken, and the derivatives are approximated as finite differences by analyzing the motion pictures. The carbon dioxide-water system is well suited for gas absorption studies with motion pictures. Its physical properties are well known, carbon dioxide is highly soluble in water and the system satisfies Henry's law for the investigated pressures. These characteristics allow the time derivatives, particularily dV/dt in equation (9) to be readily solved.

Another approach which does not involve use of photographic investigations may be taken for solution of differential equations (1) and (2):

$$\frac{dn}{dt} = -K_L a \ (C_{AS} - C_{A\infty}) \tag{1}$$

$$\frac{dz}{dt} = -V_o \tag{2}$$

these equations may be solved numerically if the functional forms of the right hand sides of equations (1) and (2) are known. The bubble surface, a, can be calculated by assuming the bubble to be a perfect sphere. C_{AS}, the bubble's equilibrium concentration, is calculated from Henry's law.

The bubble rise velocity V_o may be determined from a force balance on a spherical bubble as [22]:

$$V_o = \left[\frac{4d \ (\rho_L - \rho_g) \ g}{3 \ C_D \rho_L} \right]^{1/2} \tag{10}$$

where d is the bubble's diameter, ρ_L and ρ_g, are the liquid and gas densities respectively and g is the gravitational constant. C_D, the drag coefficient, may be evaluated using theoretical values of a sphere. The values of C_D have been found to deviate from theory for bubble diameters greater than 0.3 cm; these values have been larger than those predicted by theory. [13]

K_L, the convective mass transfer coefficient, is a function of flow conditions (Reynold's number, Re) and relative diffusivities (Schmidt's number, Sc). Previous workers [4, 21] have found that the Frossling equation for a sphere describes mass transfer for bubbles less

than 0.1 cm in diameter, and that the Higbie equation holds for bubble diameters greater than 0.3 cm in diameter. Hamerton and Garner, and Weiner have presented correlations for bubble diameters in the range of $0.1 < d < 0.3$ cm. This bubble size range has been designated as the transition region by Weiner.

The Frossling equation has been employed to describe mass transfer in pure liquids when bubbles act as spheres (diameter less than 0.1 cm) and in cases where the presence of contaminants prevented bubble circulation:

$$Sh = 2.0 + 0.55Re^{1/2} Sc^{1/3} \qquad (11)$$

where Sh, the Sherwood number is a dimensionless parameter containing K_L. The Frossling equation for spheres is a semiempirical relationship which combines two distinct contributions to the overall mass transfer. The first term, 2.0, is the contribution from molecular diffusion and can be derived by considering counterdiffusion in a stagnant medium. The second term, $0.55Re^{1/2}Sc^{1/3}$, is the contribution due to convective transfer into a moving stream; it is the result of a best fit to experimental data and theoretical considerations. Other investigators have proposed empirical correlations of the form:

$$Sh = 2.0 + C_1Re^{1/2}Sc^{1/3} \qquad (12)$$

where variations of C_1, a constant, are due to differences of experimental fit. Table 1 [Appendix] summarizes these experimental correlations for forced convection from single spheres.

Natural convection may also have a role in the total mass transfer. According to Garner and Keey, the effects of natural convection are

negligible if the Reynolds number satisfies the expression [18]:

$$Re > 0.4Gr^{1/2}Sc^{-1/6} \qquad (13)$$

where Gr, the Grashof number, is a dimensionless parameter used in natural convection correlations. Calculation of Re, Sc, and Gr for the bubble diameters studied in this investigation shows natural convection effects to be negligible. [Appendix]

The Higbie equation is based upon penetration theory with an exposure time equal to the bubble's equivalent diameter divided by the bubble's rise velocity. [9] In terms of Sh, the Sherwood number, the Higbie relation is: [Appendix]

$$Sh = 1.13\ (ReSc)^{1/2} \qquad (14)$$

This equation has been successfully used to describe mass transfer for bubbles of diameter greater than 0.3 cm.

Hamerton and Garner, [8], and Weiner, [21], both present correlations for bubbles where the diameters were in the size range of $0.1 < d < 0.3$ cm. Both correlations show excellent agreement and are based on experimental fit of data. The mass transfer expressions are:

$$Sh = 0.8\ Re \qquad \text{Weiner} \qquad (15)$$

$$Sh = 0.11\ ReSc^{1/3} \qquad \text{Hamerton \& Garner} \qquad (16)$$

The Sc number for a carbon dioxide-water system is equal to 432; $Sc^{1/3}$ is equal to 7.4. The Sc number is constant for the given gas-water system, and substitution of the $Sc^{1/3}$ term into Hamerton and Garner's expression yields:

$$Sh = 0.814\ Re \qquad (17)$$

The general form of all the presented correlations is:

$$Sh = f(Re) \qquad (18)$$

Equation (18) states that the Sherwood number is solely a function of Reynold's number, or flow conditions. However, several investigators have found that K_L also exhibits a time dependent behavior. [3,7,13,14] This time dependent behavior has been explained by two different theories.

Leonard [14] has postulated that for a highly soluble gas, the bulk liquid must migrate to the contracting bubble surface, and this liquid motion retards mass transfer away from the interface. Mass transfer is reduced by reducing the concentration gradient in the liquid film.

Another explanation for the time dependent behavior of K_L is that trace amounts of surface active agents accumulate on the bubble surface. These agents retard surface flow and reduce the mass transfer rate. [7, 13, 14]

Upon bubble formation and ascent, liquid flow around the bubble will create shear forces at the bubble surface and set up internal circulation within the bubble. At the bubble surface, liquid elements will flow around the bubble perimeter, adjacent to the circulating gas. Prior to substantial accumulation of surfactants, the bubble surface will be mobile; that is, it is capable of rapid movement and distortion. Bubble distortion will stem from mass transfer out of the bubble, and momentum effects of gas and liquid motion (i.e., turbulent liquid eddies). The microscopic fluctuations of a mobile interface create a condition of continuous surface renewal. These fluctuations cause the liquid to flow and yield to the bubble shape and exposes

fresh liquid elements to the gas.

During bubble ascent, surface active agents will first accumulate at the frontal zone of the bubble and be swept to the bubble's rear zone by liquid shear forces. Eventually, agents accumulate over the entire surface and reduce the shear forces to such an extent as to stop internal circulation. The agents will act as a buffer layer between the gas and flowing liquid and add rigidity to the bubble interface. This results in a larger overall resistance to mass transfer and reduced concentration gradient in the liquid film. [14, 7] After surface active agents reach a saturation level, the bubble's interface is no longer mobile. This state of the interface behaves similar to that of a sphere. Accordingly, Frossling's equation can be then used to describe the mass transfer from the bubble.

At the molecular level, these mentioned events have a significant effect on the diffusion of gas at the gas-liquid interface and will influence the overall rate of mass transfer from the bubble. Although the general effects of surface active agents in known, mass transfer theory has not satisfactorily described or predicted the effects with accepted concepts. Since all industrial applications involve surface active agents within the liquid, mass transfer in real liquids must account for the effects of these agents. The author believes this can be done by using a time dependent mass transfer coefficient, K_L. The time dependent behavior of K_L may be explained using the concept of critical time. The critical time concept relates to the accumulation of surface active agents on the bubble. This concept can be developed

if the following assumptions are made:

1. The concentration of the surface active agents in the liquid is uniform.
2. The rising bubble captures all the surfactant that comes in contact with the bubble's projected area.
3. The bubble's diameter and rise velocity are constant.

The hypothetical volumetric rate of liquid which comes in contact with the bubble is given by the expression:

Volumetric rate of liquid contact

= (projected area) • (bubble rise velocity)

= cm^2 • cm/sec

= cm^3/sec.

The rate of surfactant captured by the surface is then:

$$\left[\begin{array}{c}\text{Surfactant}\\ \text{capture}\\ \text{rate}\end{array}\right] = \left[\begin{array}{c}\text{Volumetric rate}\\ \text{of liquid}\\ \text{contact}\end{array}\right] \cdot \left[\begin{array}{c}\text{Surfactant}\\ \text{concentration}\\ \text{in liquid}\end{array}\right]$$

Based upon the three assumptions, this surfactant capture rate will be constant and the total amount of surfactant on the surface will be directly dependent on time:

$$\left[\begin{array}{c}\text{Total surfactant}\\ \text{on bubble}\\ \text{surface}\end{array}\right] = \left[\begin{array}{c}\text{Surfactant}\\ \text{capture}\\ \text{rate}\end{array}\right] \cdot \left[\begin{array}{c}\text{Time}\end{array}\right] \qquad (19)$$

$$= \text{moles/sec} \cdot \text{sec}$$

$$= \text{moles}$$

where the time is measured from the initial release of the bubble into the liquid pool, or the bubble age.

If a critical time, t_c, is defined as the time required for surfactant to accumulate upon the bubble surface, and completely cover the bubble, or reach a saturation level, the amount of surfactant at any time can be evaluated by equation (19). The critical time concept also infers that there will be two different mass transfer mechanisms at the bubble surface: the mass transfer prior to t_c when the total surfactant is increasing, and mass transfer at t_c and after, when the surfactant level has reached its saturation level and remains constant.

In modeling real systems, the mass transfer coefficient for time greater than or equal to t_c was evaluated by Frossling's equation. For any bubble with a diameter in the transition region, the mass transfer coefficient for time less than t_c was evaluated using a combination of Frossling's equation and Hamerton and Garner's transition equation. During this time period a changing weight factor was assigned to the contribution by each correlation and the total mass transfer was taken as the sum of the two contributions. The weight factors were based upon a relative time, t/t_c, and were linear with respect to time as shown by equation (19). The contributions to mass transfer during this time period are:

$$\text{Transition contribution} = (1 - t/t_c)\ Sh_{transition} +$$

$$\text{Frossling contribution} = (t/t_c)\ Sh_{Frossling}$$

$$Sh_{total} = (1 - t/t_c)\ Sh_{transition} + (t/t_c) Sh_{Frossling} \qquad (20)$$

This assignment of weight factors implies that bubble interface without surface active agents is mobile, and that the portion of

interface covered by agents is immobile. A correlation factor, $\bar{\alpha}$, [12] has been used to account for the effects of surface active agents on mass transfer but this parameter does not consider the mechanism which inhibits mass transfer.

Figure 1

MODEL: SINGLE RISING GAS BUBBLE IN LIQUID

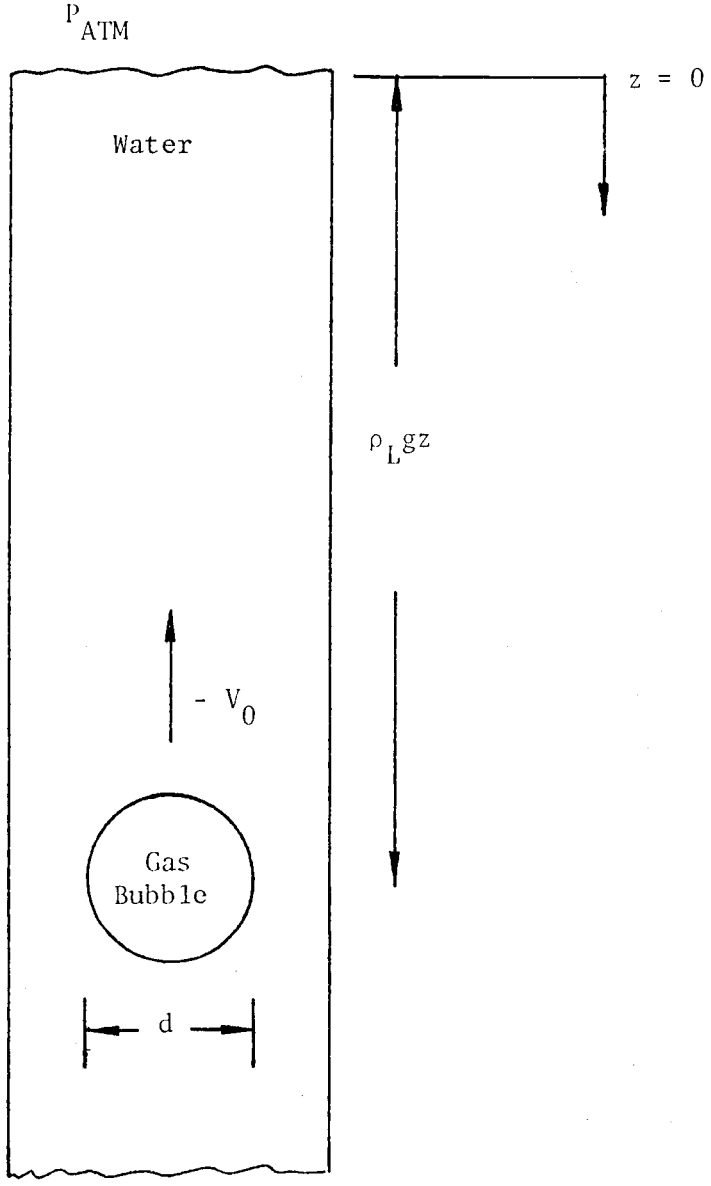

III. INSOLUBLE GAS CASE

The simplest case of a bubble rising in a fluid serves as a starting point for analysis. This case consists of a single spherical insoluble gas bubble rising in a liquid column. Solution is directed toward description of a bubble's size and gas concentration. The applicable assumptions in the derivation of equation (9) are used again. These assumptions are:

1. The gas is ideal.
2. Humidification and counterdiffusion effects are negligible.
3. Surface tension effects are negligible.

The bubble's initial diameter and position fixes the moles present in the bubble by:

$$n = \frac{PV}{RT} = \frac{(P_{ATM} + \rho_L g z)\pi d^3}{6RT} \tag{21}$$

The moles of gas, n, are constant and the bubble's volume at any subsequent position is:

$$V = \frac{nRT}{P} = \frac{nRT}{P_{ATM} + \rho_L g z} \tag{22}$$

The diameter of the bubble is evaluated with the assumption that the bubble is a perfect sphere:

$$d = \left[\frac{6V}{\pi}\right]^{1/3} = \left[\frac{6nRT}{(P_{ATM} + \rho_L g z)\pi}\right]^{1/3} \tag{23}$$

The surface area of the bubble is:

$$a = \pi d^2 = \left[\frac{6nRT}{P_{ATM} + \rho_L g z}\right]^{2/3} \pi^{1/3} \tag{24}$$

The gas concentration in the bubble is:

$$C_A = \frac{P}{RT} = \frac{P_{ATM} + \rho_L g z}{RT} \qquad (25)$$

After stipulating the initial size and position of the bubble, the volume and gas concentration of the bubble at any other specified condition can be calculated.

The next level in analysis involves relaxing the insoluble gas restriction. Analysis becomes more complex when considering the general case of mass transfer from a single rising spherical bubble and numerical methods are employed for solution of this case.

IV. COMPUTER MODEL DISCUSSION

As shown in the theoretical considerations section, the evaluation of equation (1) requires a mass transfer coefficient value, K_L, which is a function of the bubble rise velocity. In turn, the evaluation of the bubble rise velocity by equation (10) requires the diameter of the bubble which can be evaluated only after equation (1) has been solved. Equation (2) is also a function of the bubble rise velocity. Due to the interdependency among the equations, the differential equations (1) and (2) must be solved simultaneously by numerical integration techniques.

Three numerical methods, Euler's, Runge-Kutta, and Regula-Falsi have been used for solving differential equations (1) and (2). The Euler's and the Runge-Kutta methods were used to calculate the position of the bubble and the moles of gas present in the bubble at any time. These two single step methods provide a solution to a differential equation if an initial condition is known. The Regula-Falsi method, an iterative technique used to solve for the root of an equation, was applied to determine accurate values of a bubble rise velocity at any diameter and position [Appendix]. The values of the bubble rise velocity obtained using the Regula-Falsi method were used in the Euler's and the Runge-Kutta solutions of equations (1) and (2).

Initially, the Euler's method was selected since it permitted an easy check of the solution through hand calculations of initial iterations. A Runge-Kutta-Merson routine, which is a fourth-order Runge-Kutta alogarithm with logic incorporated to adjust the step size

in order to maintain desired accuracy, was used exclusively in the final solution of equations (1) and (2) after the technique was validated by comparing its solution to the Euler's solution.

The Regula-Falsi method is used to solve for the root of an equation. The bubble rise velocity function, equation (10), may be altered to a new functional form such that the root of this new form will be the bubble rise velocity [Appendix]:

$f(V_o) = 0$, V_o = rise velocity

This application of the Regula-Falsi method uses four subprograms in calculation of a bubble rise velocity. A bubble rise velocity will be a function of the diameter of the bubble, bubble and liquid density difference, and bubble drag coefficient. When the diameter and position of the bubble are known, SUBROUTINE END will approximate the bubble rise velocity by an upper and lower value of rise velocity. These upper and lower bounds of velocity are used by FUNCTION RISE to initiate the Regula-Falsi iteration scheme. FUNCTION RISE converts the velocity values into a functional form that is compatible with the Regula-Falsi method. FUNCTION DRAG calculates a drag coefficient for any bubble Reynold's number. These drag coefficients are called and used by FUNCTION RISE. FUNCTION REGULA calls FUNCTION RISE and performs the Regula-Falsi iteration until the rise velocity function converges to zero. Upon satisfaction of the convergence criteria, the accurate value of bubble rise velocity is transferred for use in either the Euler's or Runge-Kutta methods.

Figure 2

THEORETICAL BUBBLE RISE VELOCITIES VERSUS BUBBLE DIAMETER

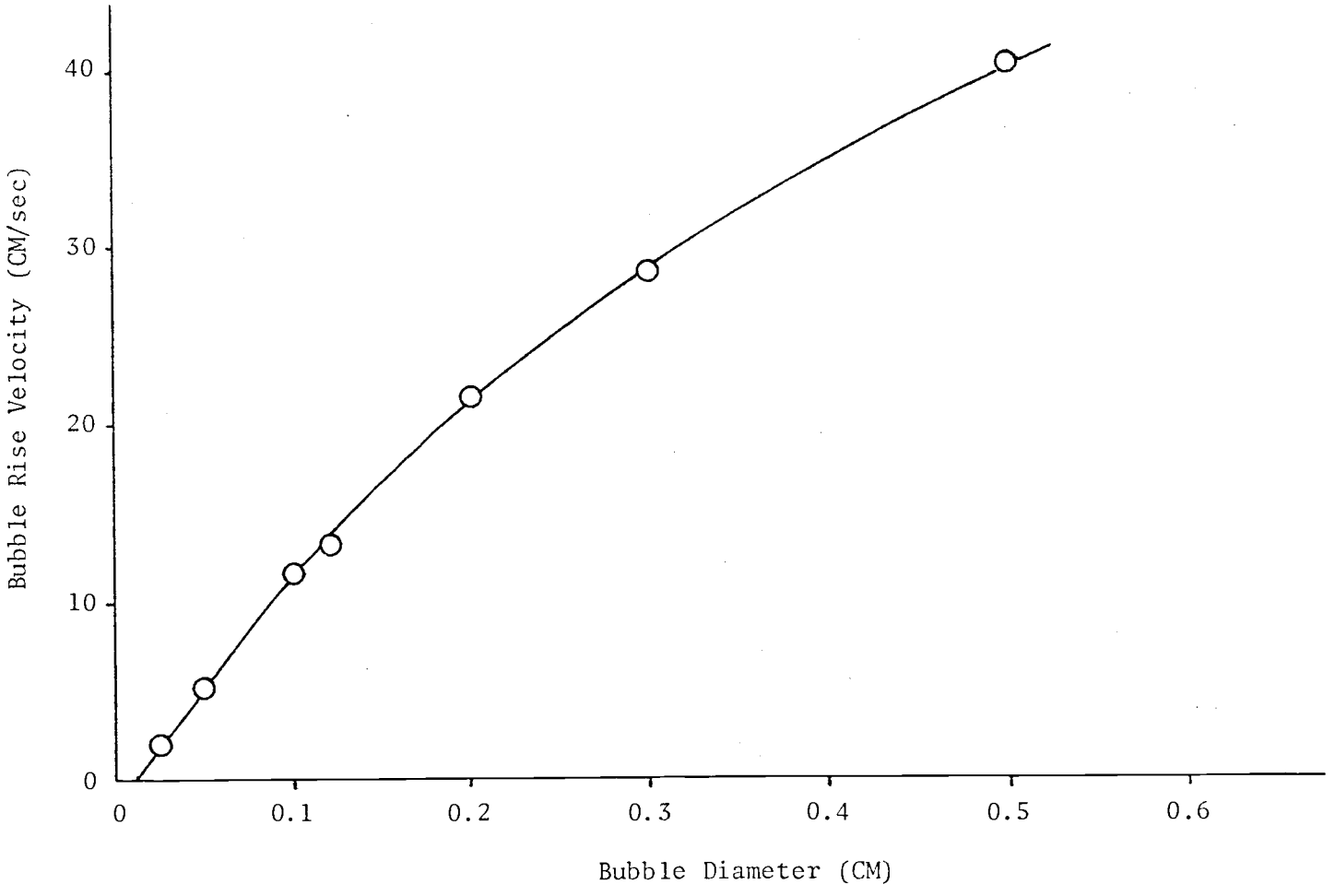

Figure 3

BUBBLE RISE VELOCITY FLOWSHEET

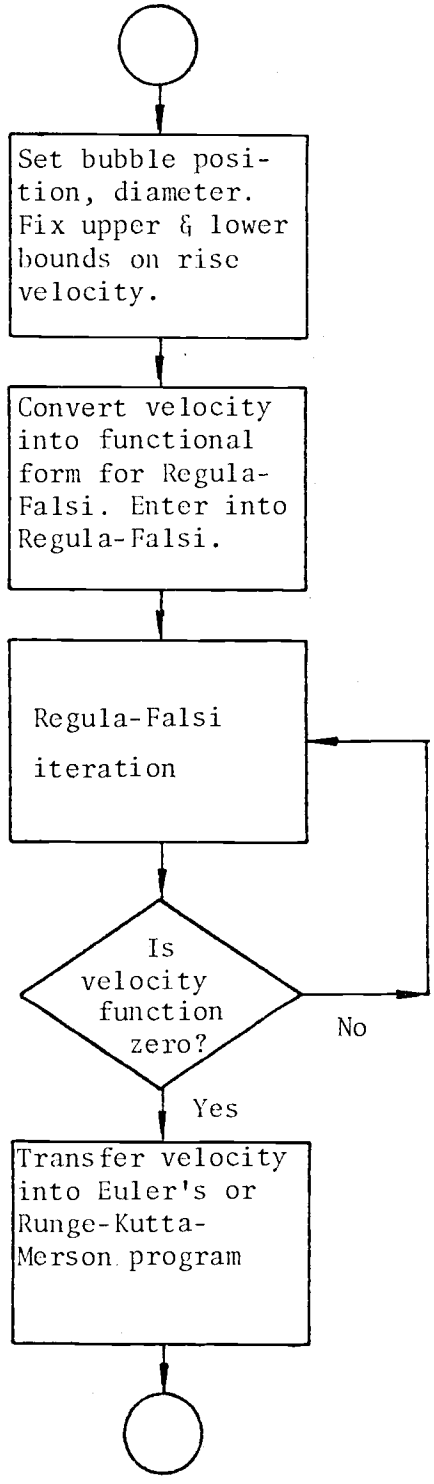

The behavior of many physical processes, particularly those in systems undergoing time-dependent changes, can be described by ordinary differential equations. This development will be restricted to first-order ordinary differential equations which are by definition, of the form [1]:

$$\frac{dY}{dX} = f(X,Y) \tag{26}$$

Systems of first-order ordinary differential equations are of the form:

$$\begin{aligned}
\frac{dY_1}{dX} &= f_1(X, Y_1, Y_2, \ldots Y_n) \\
\frac{dY_2}{dX} &= f_2(X, Y_1, Y_2, \ldots Y_n) \\
&\cdot \\
&\cdot \\
\frac{dY_n}{dX} &= f_n(X, Y_1, Y_2, \ldots Y_n)
\end{aligned} \tag{27}$$

A solution Y(X) is desired which satisfies equation (26) and an initial condition. In general, it is impossible to obtain an analytical solution to equation (26). Instead the interval in the independent variable X over which the solution is desired, [a,b] is divided into subinterval or steps. The value of the true solution, Y(X) is approximated at n + 1 evenly spaced values of X, (X_0, X_1, X_2 ... X_n), so that the step size h is given by:

$$h = \frac{b-a}{n} \tag{28}$$

and

$$X_i = X_0 + ih, \quad i = 0, 1, 2, \ldots n \tag{29}$$

Thus the solution, Y(X) is given as tabular values for discrete values of X only.

Let the true solution of Y(X) be denoted as $Y(X_i)$ and computed approximation of Y(X) at these same points be denoted Y_i so that

$$Y_i \simeq Y(X_i) \tag{30}$$

The true derivative dY/dX at any X_i will be approximated by $f(X_i, Y_i)$ so that:

$$f(X_i, Y_i) \simeq f(X_i, Y[X_i]) \tag{31}$$

When the numerical calculations are done exactly, that is without roundoff error (see below), the difference between the computed Y_i and true value $Y(X_i)$ is termed the discretization or truncation error, e_i:

$$e_i = Y_i - Y(X_i) \tag{32}$$

The local discretization error encountered in integrating a differential equation across one step is sometimes called the local truncation error. The discretization error is determined solely by the particular numerical solution procedure selection; this type of error is independent of computing machine characteristics.

An inherently different kind of error results from computer design. In practice, computers have a finite memory, and the number of digits retained for a number by the computer is fixed. Thus any number with more significant digits than can be retained must be

approximated by "rounded" values. This error is termed roundoff and is determined by the computing characteristics of the machine. Some upper bound can usually be found for truncation error of a particular numerical method. Roundoff error, on the other hand is extremely complex and unpredictable.

Common numerical alogarithms used for solving first order ordinary differential equations with an initial condition are often based upon direct or indirect use of Taylor's expansion of the solution function Y(X). A Taylor's series expansion of Y(X) about some starting point X_0 is:

$$Y(X_0 + h) = Y(X_0) + hf(X_0, Y(X_0)) + \frac{h^2}{2!} f'(X_0, Y(X_0)) + \frac{h^3}{3!} f''(X_0, Y(X_0)) + \ldots \tag{33}$$

where $f'(X, Y(X)) = d/dX\ [f(X,Y(X))]$

and $f''(X,Y(X)) = d^2/dX^2[f(X,Y(X))]$

If $Y(X_0)$ is specified as the initial condition, $f(X_0, Y(X_0))$ can be computed directly from the differential equation:

$$\frac{dY}{dX} = f(X,Y) \tag{26}$$

Similiarly, alogarithms for stepping from X_i to X_{i+1} can be based upon the Taylor's expansion of Y(X) about X_i:

$$Y(X_{i+1}) = Y(X_i) + hf(X_i,Y(X_i)) + \frac{h^2}{2!} f'(X_i,Y(X_i)) + \frac{h^3}{3!} f''(X_i,Y(X_i)) + \ldots + \frac{h^n}{n!} f^{(n-1)}(X_i,Y(X_i)) + \frac{h^{n+1}}{(n+1)!} f^{(n)}(\xi,Y(\xi)) \tag{34}$$

where ξ is in the interval (X_i,X_{i+1})

Unfortunately, in the general case, the differentiation of f(X,Y) becomes enormously complicated. Except for the simplest case,

$$Y(X_{i+1}) = Y(X_i) + hf(X_i, Y(X_i)) + O(h^2) \tag{35}$$

The direct Taylor's expansion of equation (34) is not often used. Here "$O(h^2)$" means the maximum local truncation error is of order 2. In general "O( )" means terms of order ( ) and is used to estimate local and overall truncation error.

Euler's method is a single step method that solves first order differential equations by calculation of one derivative per step. The general form of a first order differential equation is:

$$\frac{dY}{dX} = f(X,Y) \tag{26}$$

and Euler's alogarithm assumes the form:

$$Y_1 = Y_0 + hf(X_0, Y(X_0)) \tag{35a}$$

$$Y_{i+1} = Y_i + hf(X_i, Y(X_i)) \qquad i \geq 1 \tag{35b}$$

where h is the step size used by Euler's method.

There is a simple geometric interpretation for equation (35b). The solution across the interval (X_0, X_1) is assumed to follow the line tangent to Y(X) at X_0. (See Figure 5) When Euler's method is applied repeatly across several intervals in sequence, the numerical solution traces out a polygon segment with sides of slopes f_i, i = 0,1,2,3...n-1. [1]

The maximum local truncation error computed from a Taylor expansion term is:

$$e_t = \frac{h^2}{2!} f'(\xi, Y(\xi)) \text{ where } \xi \text{ is in the interval } (X_i, X_{i+1}) \tag{36}$$

where the local truncation error is proportional to h^2.

A detailed error analysis using Euler's method is given in numerical methods books [1]. The result presented without derivation stipulates that the total truncation error is proportional to h:

$$e_{total} = Y_i - Y(X_i) = 0(h) \qquad (37)$$

Note that the local truncation error is of order h^2 but the total truncation error is of order h.

Local truncation error, e, may be expressed as absolute error $|e|$, or as a percent of the current value of the dependent variable, Y. (i.e., $\%e = |e/Y| \times 100$, termed percent or relative error)[5]. Once the truncation error has been specified, it is used in estimation of the accuracy or the reliability of a numerical solution.

A main program, EULER, utilized Euler's method for solution of equations (1) and (2). Program EULER called subprograms END, RISE, DRAG, and REGULA in determination of accurate values of rise velocity. Subprograms CONV and CONC were called to calculate convective mass transfer coefficients, K_L, and equilibrium concentrations, C_{AS}, respectively. Subprograms MAIN and BUBBLE were used to enter initial bubble conditions and calculate initial bubble characteristics, respectively.

The system of equations (1) and (2) have dependent variables with differences in order of magnitude of approximately 10^8. (i.e., $10^{-7} < n < 10^{-9}$ moles and $0 < z < 450$ cm). Thus use of an absolute truncation error of magnitude e equal to 0.0001 per step would be appropriate for equation (2) but inappropriate for equation (1) because e is several orders of magnitude greater than n. Use of a relative error criteria in the Euler's method program showed that the relative error in z was always larger than the relative error in n at a given step size in t. With this relationship between relative error in equations (1) and (2), then an absolute truncation error in z was specified with assurance that the absolute truncation error in n was satisfactorily small. Stated another way, equation (2) was the stiffer of the two equations and would set the step size necessary to maintain a desired solution accuracy.

Speece [19] had previously solved equation (1) for the oxygen-water system by converting the differential equation into

a finite difference equation. In addition, the bubble rise velocity was set equal to a constant and the convective mass transfer relationship was simplified. His numerical solution represents the use of Euler's method and unfortunately no mention was made of his truncation error or of the error criteria used. As a result, the validity of his solution is unknown.

Figure 4

EULER'S METHOD FLOWSHEET

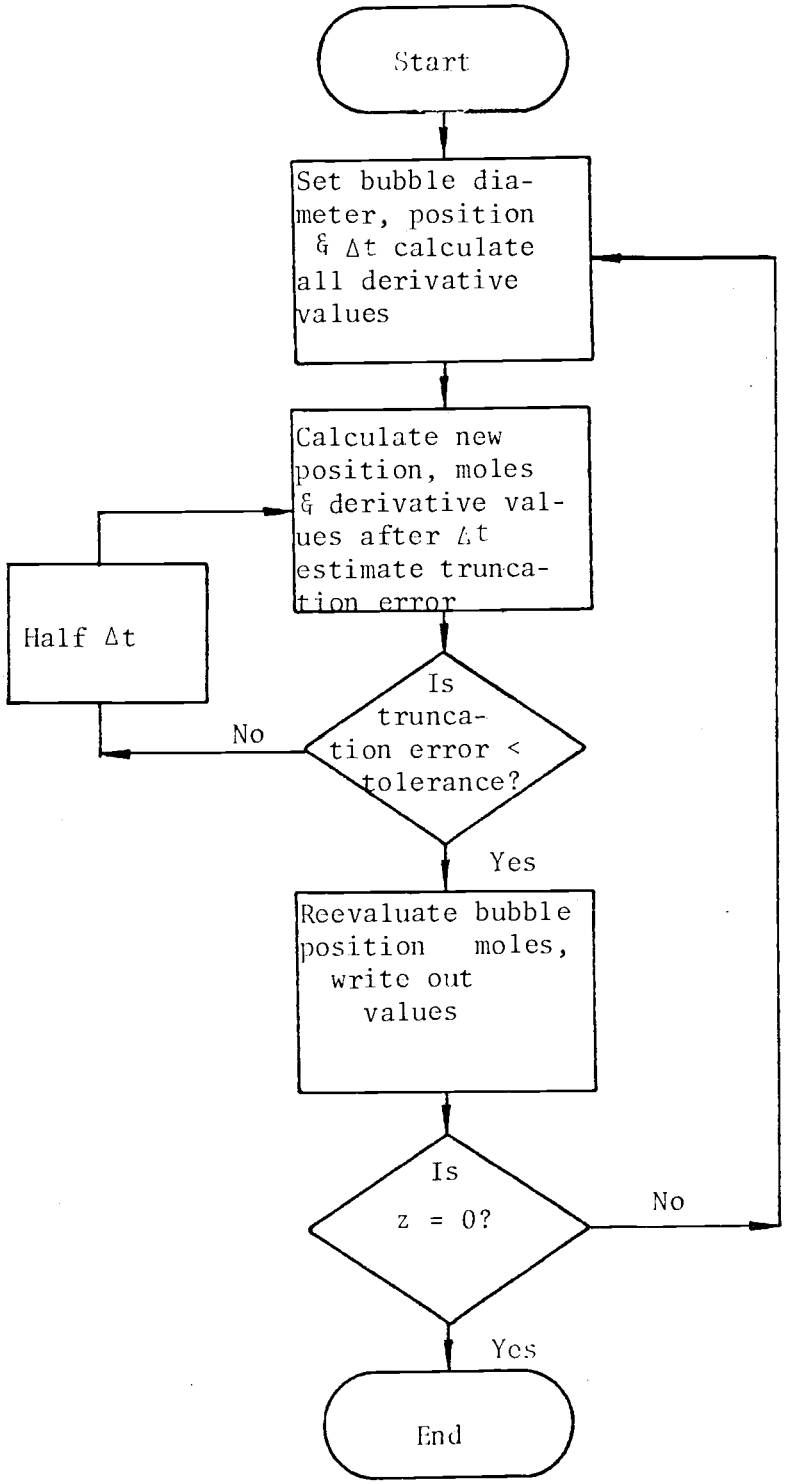

Figure 5

GRAPHICAL INTERPRETATION OF EULER'S METHOD

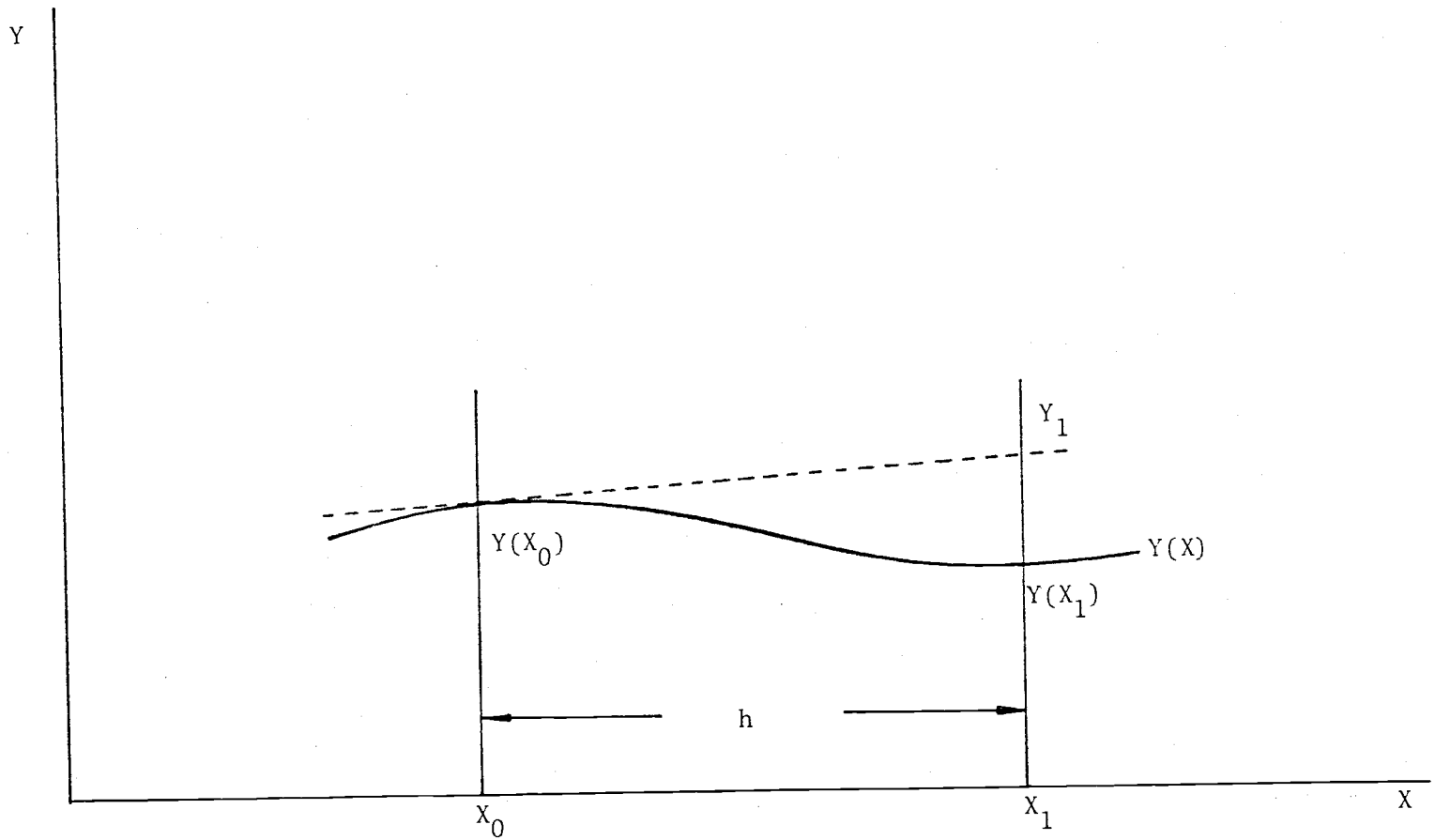

The solution of a differential equation by direct Taylor's expansion of the object function is generally not practical if derivatives of higher order than the first are retained. For all but the simplest equations, the higher-order derivatives become quite complicated.

Fortunately it is possible to develop one step procedures which involve only first-order derivative evaluations, but which also produce results equivalent in accuracy to the higher-order Taylor's formulas. These alogarithms are called the Runge-Kutta methods. Approximations of the second, third and fourth order, (that is, approximations that have an accuracy equivalent to Taylor's expansions, retaining terms in h^2, h^3, and h^4, respectively) require the estimation of f(X,Y) at two, three and four values, respectively, of X on the interval $X_i<X<X_{i+1}$.

All the Runge-Kutta methods have alogarithms of the form:

$$Y_{i+1} = Y_i + h\phi\ (X_i,\ Y_i,\ h) \qquad (39)$$

where ϕ, termed the increment function, is simply a suitably chosen approximation of f(X,Y) on the interval $X_i<X<X_{i+1}$. All the fourth-order Runge-Kutta formulas are of the form:

$$Y_{i+1} = Y_i + h(aK_1 + bK_2 + cK_3 + dK_4) + O(h^5)$$

where a,b,c and d are constants and K_1, K_2, K_3 and K_4 are approximate derivative values calculated on the interval $X_i<X<X_{i+1}$.

Program REST solves equations (1) and (2) by the Runge-Kutta-Merson alogarithm which calculates five derivatives values per step. Subprograms REGULA, RISE, END, and DRAG are called by REST in determination of accurate values of bubble rise velocity. Subprograms CONV and CONC are called by REST and used to calculate the convective mass transfer

coefficient, K_L, and the equilibrium concentration, C_{AS}, respectively. Initial bubble conditions, the bubble's position and diameter, and a critical time value are read into REST. The critical time, t_c, and time, t, are transferred into CONV for the calculation of an overall Sherwood number (Sh_{total}).

An absolute value of local truncation error, e, is specified in REST and the Runge-Kutta-Merson subroutine (by Dr. Eugene Elzy, Chemical Engineering Department, OSU) used in this model adjusts the step size to maintain the desired accuracy in both equations. An accuracy criteria of e equal to 0.001 was used. The results obtained with this criteria were found to be adequate.

Figure 6

RUNGE-KUTTA-MERSON FLOWSHEET

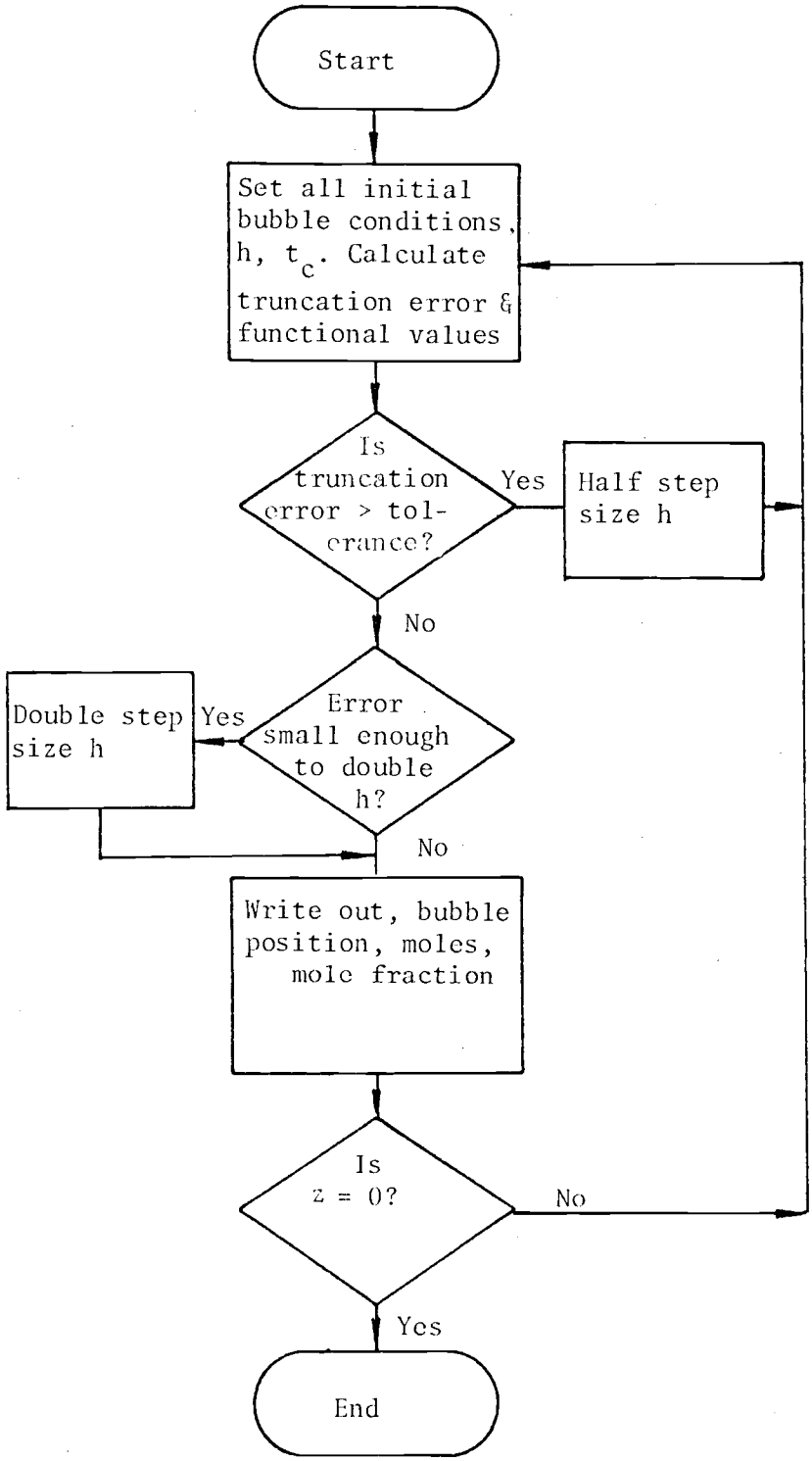

V. RESULTS

The computer model, with and without the inclusion of the critical time parameter was applied to the carbon dioxide-water system. Without the inclusion of the critical time parameter, the computer model yields results predicting much higher mass transfer rates than those shown in data of Deindoerfer. Inclusion of the critical time parameter resulted in predictions corresponding closely to data collected by three different investigators. Figures 7a, 7b, 8a, 8b, 9a, and 9b show the comparison of the computer model to the data of Deindoerfer, Garbarini, and Datta, respectively. [2,3,6] The plots include the computer model's prediction of bubble position and volume versus time and compares it to the data of the three investigations.

In the three comparisons, there is an excellent agreement between the computer model and experimental volume-time relations. However, the agreement between Garbarini's and Datta's position-time data and the computer model prediction of position-time is not as good as the comparison of volume-time relations. This poor comparison with the position-time data is undoubtedly due to the fact that both experiments involved initial bubble sizes greater than 0.5 cm in diameter. The model used theoretical values of drag coefficients which were lower than experimentally obtained drag coefficients. Experimental drag coefficients of bubbles in contaminated liquid deviate from sphere values at a bubble diameter equal to 0.3 cm, are greater than theoretical values for bubble diameters greater than 0.3 cm.

This difference in drag coefficients results in predicted rise

velocities greater than experimental rise velocities; thus this poor comparison between the predicted bubble position and experimental position should be expected. The comparison of Deindoerfer's data and the computer model indicates the adequacy of the model for bubbles having initial diameters less than 0.3 cm. In this case where the initial bubble diameter was equal to 0.285 cm the agreement between the position predicted by the model and the experimental position is excellent. Since the model uses theoretical values of drag coefficients, the use of the model to describe mass transfer for bubbles having an initial diameter greater than 0.3 cm should be done judiciously.

A critical time value of 4.0 seconds for Garbarini's and Datta's data, and a critical time of 2.0 seconds for Deindoerfer's data was used. This smaller value of t_c used with the data of Deindoerfer indicates that the water used in the Deindoerfer experiment was probably contaminated to a higher degree than the water of Garbarini or Datta. Lochiel and Calderbank also concluded that the results of Deindoerfer were due to contaminated liquid [6].

Use of a critical time of 4.0 seconds indicates that removal of all contaminants is difficult even in research situations [13]. The mass transfer coefficient, K_L, has been reported to be time dependent even in highly purified liquids; this behavior may be due to the researcher's inability to remove all of the contaminants.

The bubble's volume-time relationship or mass transfer history is a more desirable parameter than the bubble's position and time relationship, since it has a potential application in real processes.

Figure 7a

COMPARISON OF COMPUTER MODEL TO DATA OF DEINDOERFER

BUBBLE VOLUME VERSUS TIME

t_c = 2.0 seconds

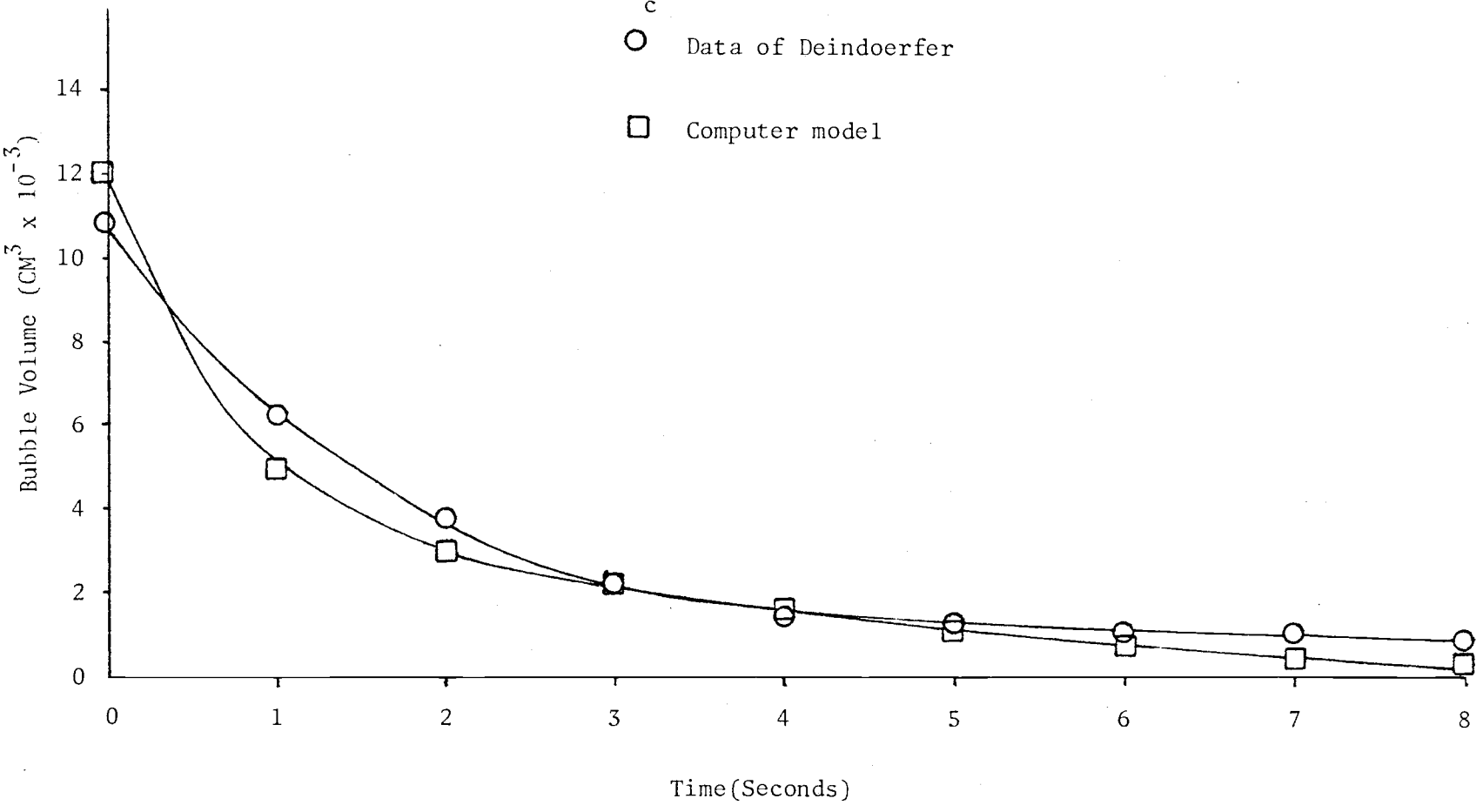

Figure 7b

COMPARISON OF COMPUTER MODEL TO DATA OF DEINDOERFER

BUBBLE POSITION VERSUS TIME

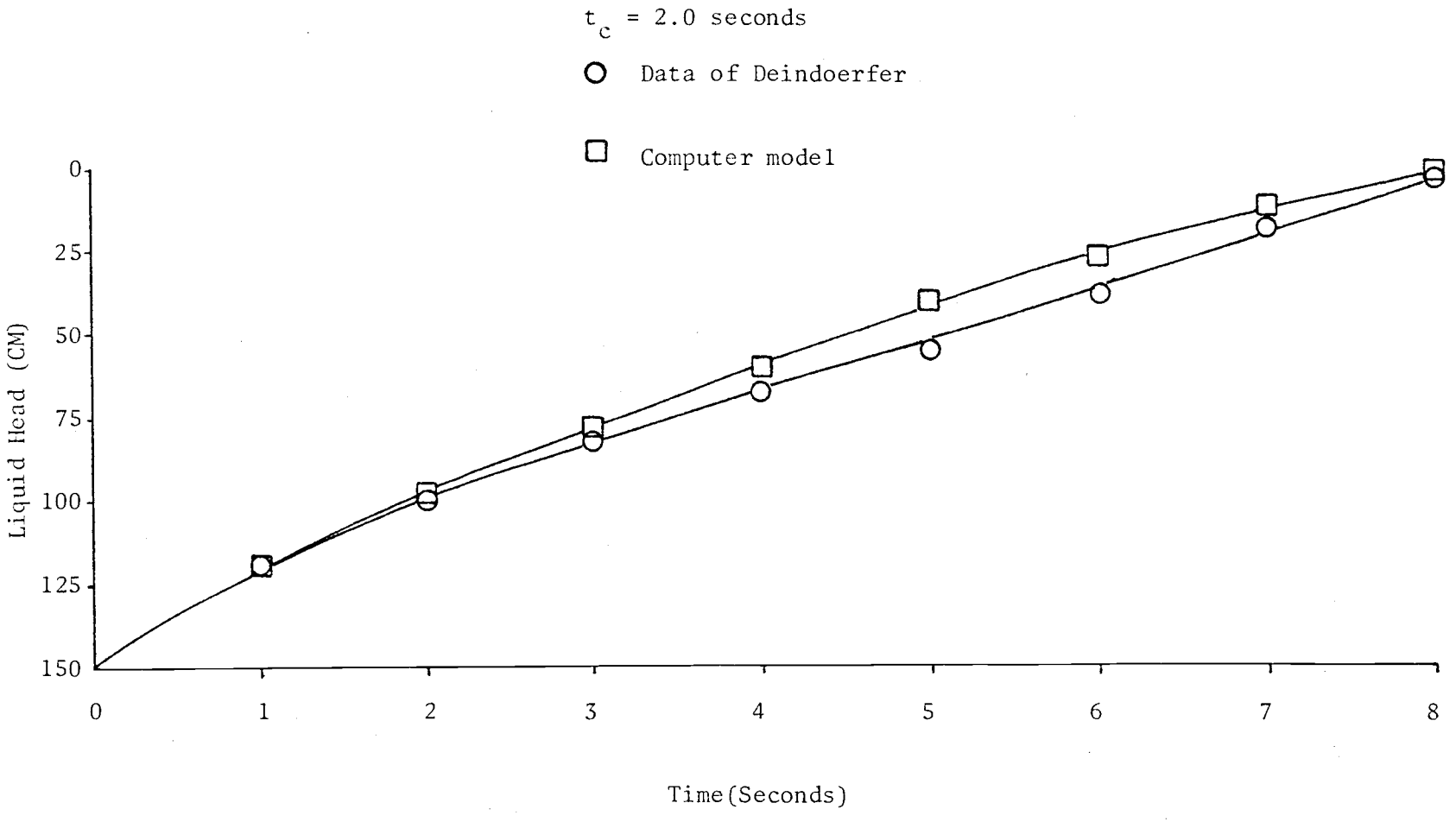

Figure 8a

COMPARISON OF COMPUTER MODEL TO DATA OF GARBARINI
BUBBLE VOLUME VERSUS TIME

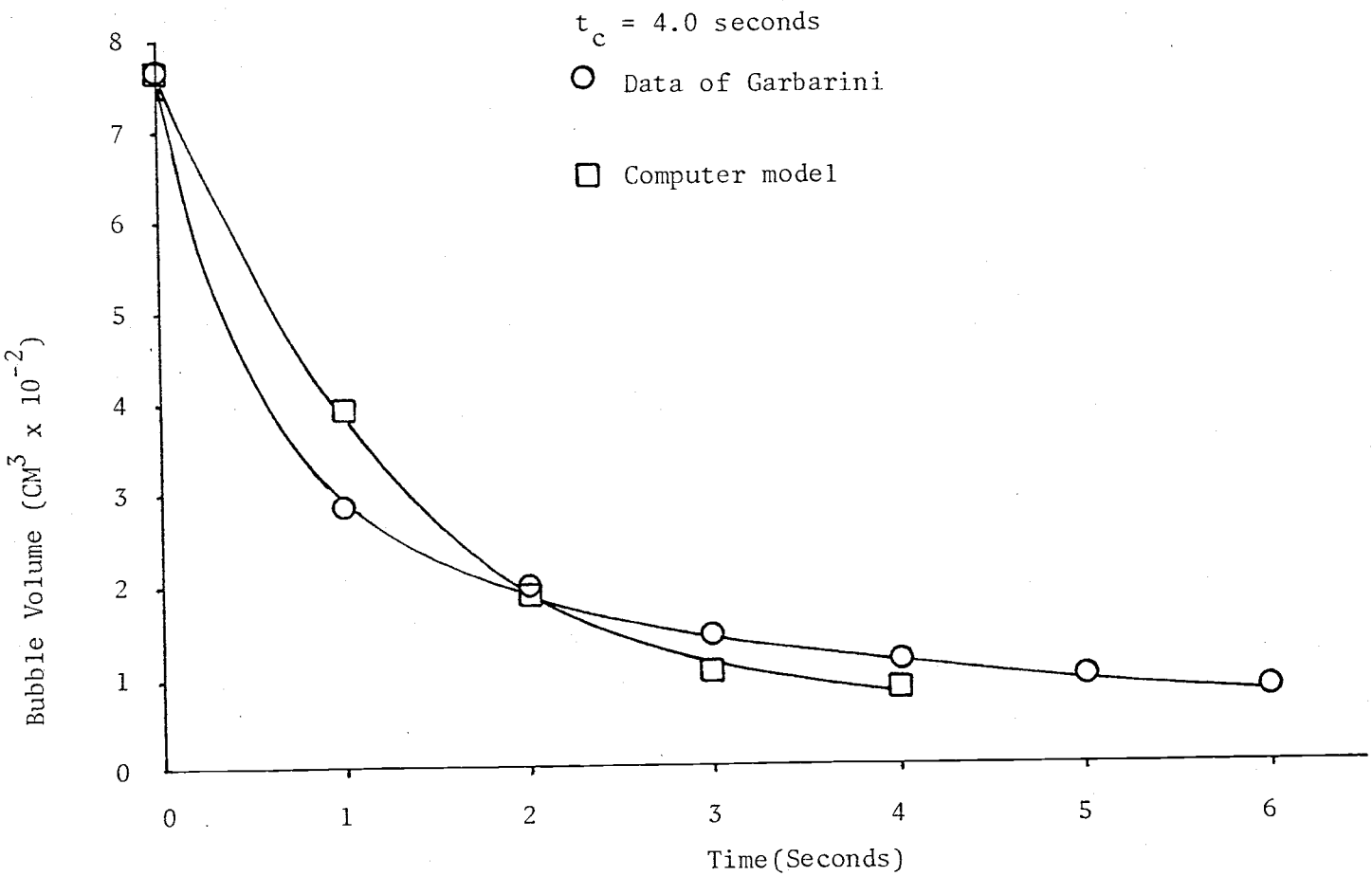

Figure 8b

COMPARISON OF COMPUTER MODEL TO DATA OF GARBARINI
BUBBLE POSITION VERSUS TIME

t_c = 4.0 seconds

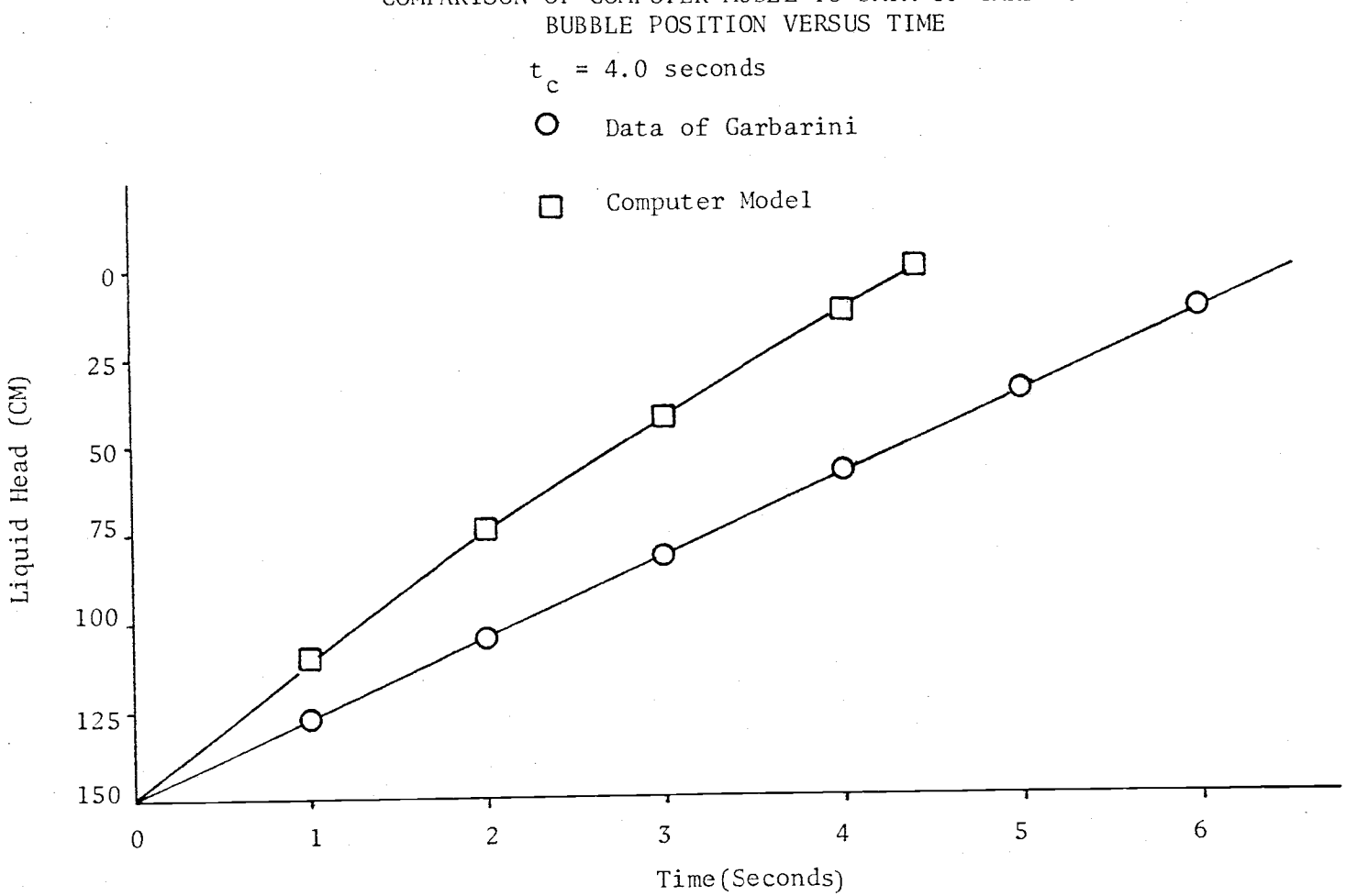

Figure 9a

COMPARISON OF COMPUTER MODEL TO DATA OF DATTA
BUBBLE VOLUME VERSUS TIME

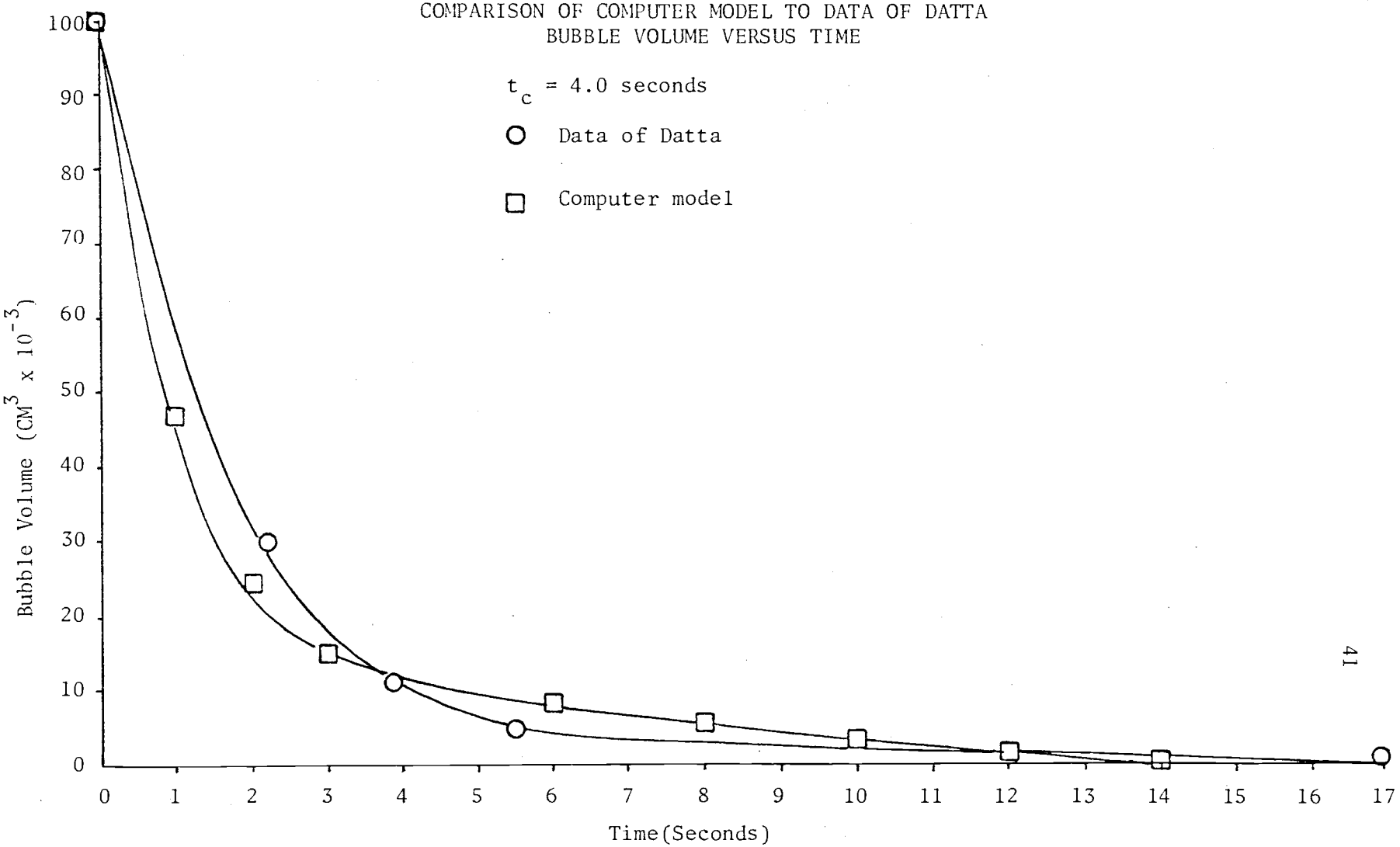

Figure 9b

COMPARISON OF COMPUTER MODEL TO DATA OF DATTA
BUBBLE POSITION VERSUS TIME

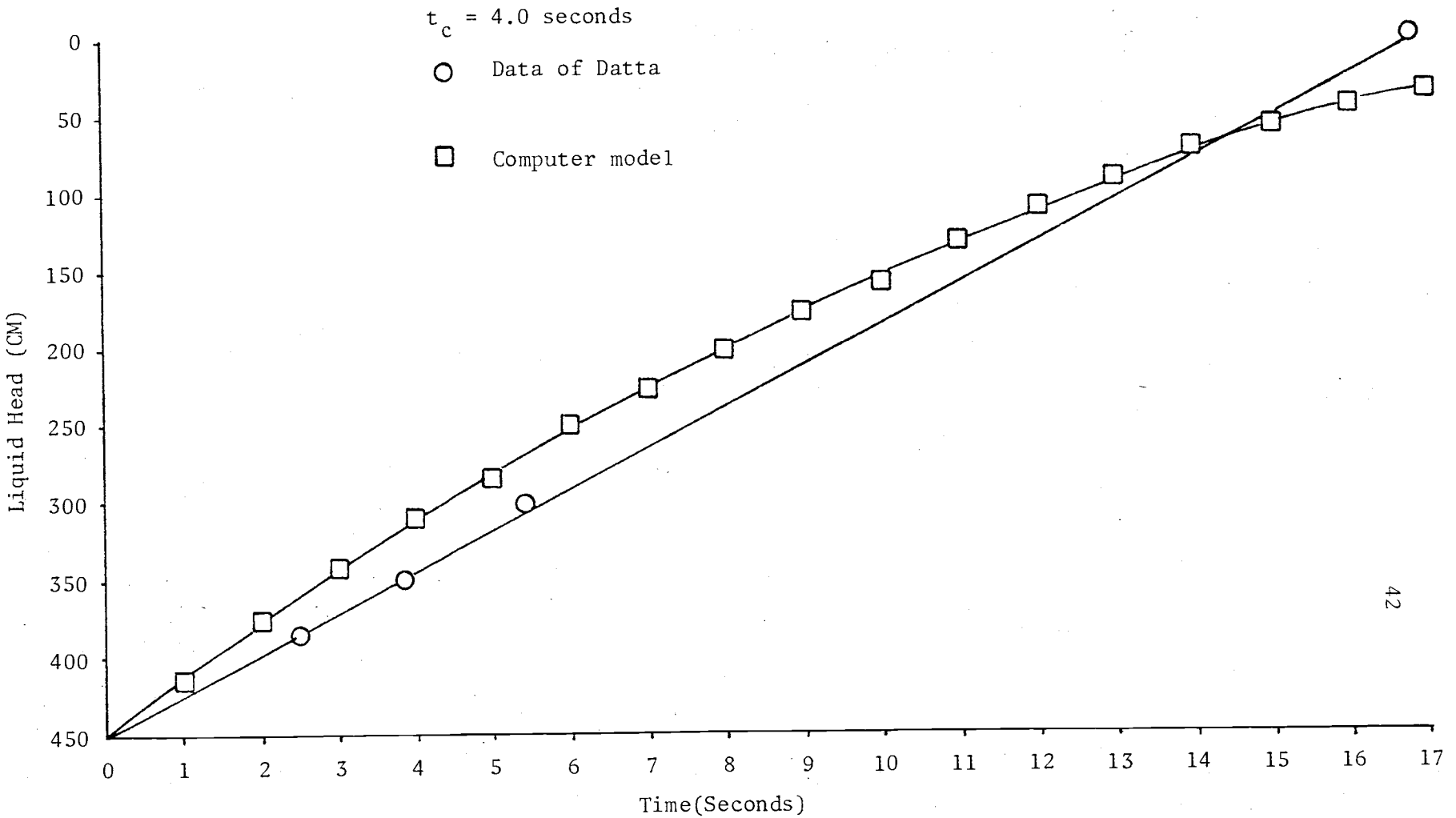

Figures 10a and 10b show the behavior of carbon dioxide bubbles in water when the initial bubble diameter is varied. A large bubble will rise and burst on the liquid surface, releasing a portion of gas to the atmosphere. A bubble of a sufficiently small diameter will virtually disappear before reaching the liquid surface. Bubbles that are very small and disappear indicate a poor design, since no mass transfer takes place in the liquid above the disappearance height. To obtain a certain amount of gas transfer, there exists an optimum bubble size that will have mass transfer occuring until the instant the bubble just reaches the liquid surface. Figure 10a also shows that the bubble surface/volume ratio has a significant role on the remaining bubble. The bubble surface contracts towards the center of the bubble at an increasing rate just prior to disappearance.

Figure 10a

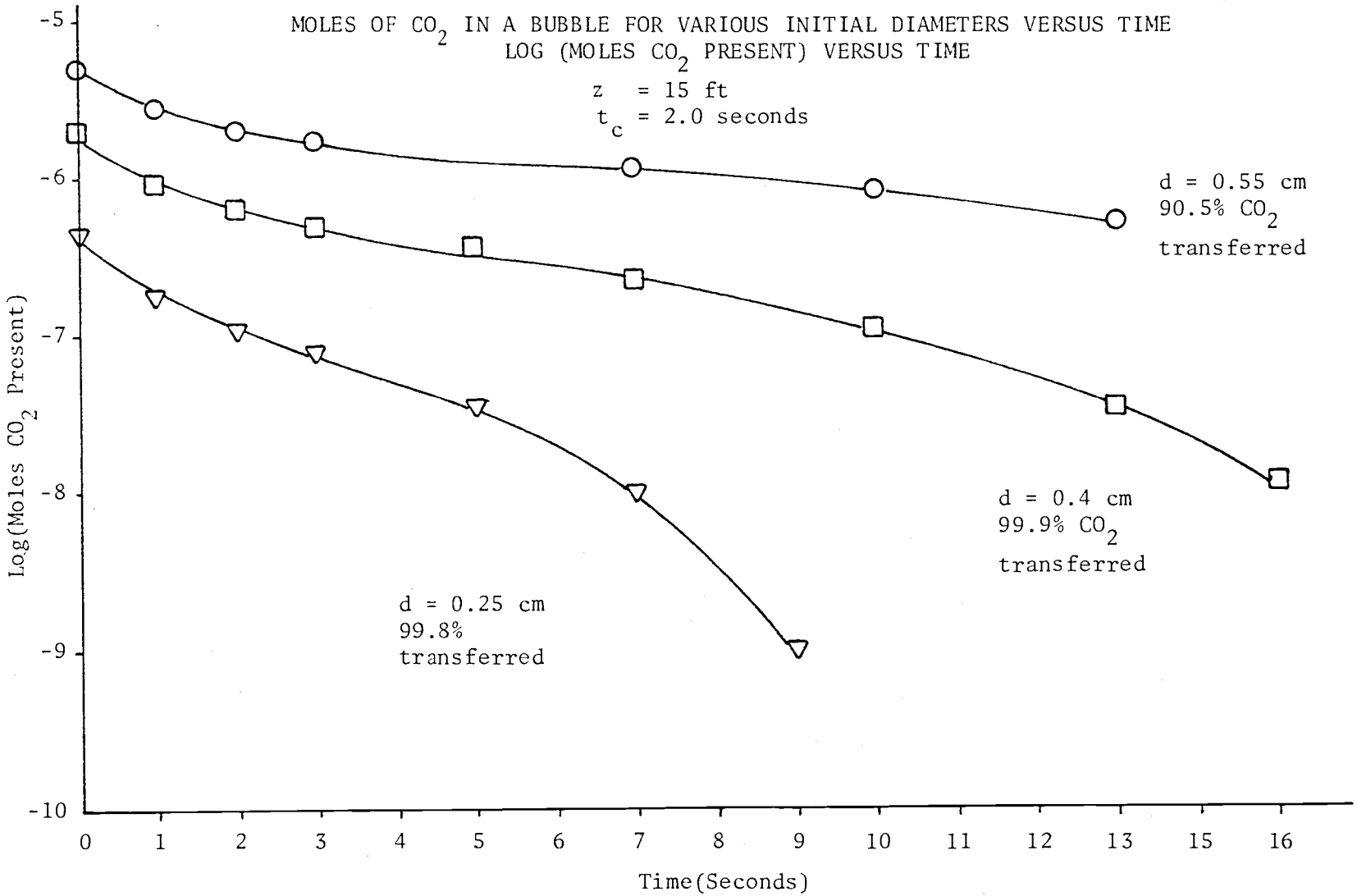
MOLES OF CO_2 IN A BUBBLE FOR VARIOUS INITIAL DIAMETERS VERSUS TIME
LOG (MOLES CO_2 PRESENT) VERSUS TIME
z = 15 ft
t_c = 2.0 seconds
d = 0.55 cm
90.5% CO_2
transferred
d = 0.4 cm
99.9% CO_2
transferred
d = 0.25 cm
99.8%
transferred
Log(Moles CO_2 Present)
-5
-6
-7
-8
-9
-10
0
1
2
3
4
5
6
7
8
9
10
11
12
13
15
16
Time(Seconds)

Figure 10b

CO_2 BUBBLE POSITION VERSUS TIME FOR VARIOUS INITIAL BUBBLE DIAMETERS

z = 15 feet

t_c = 2.0 seconds

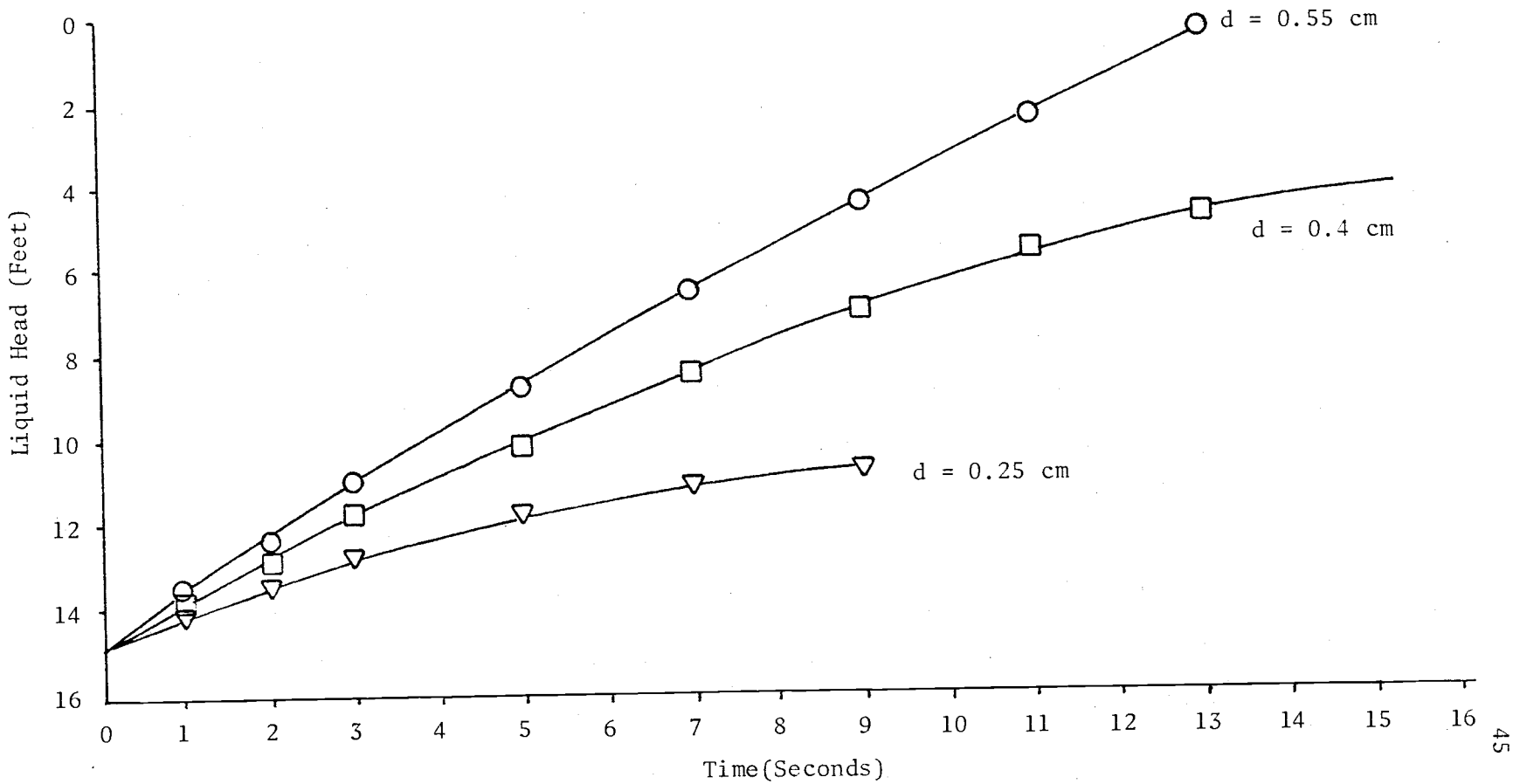

Figure 11 plots the moles present in a carbon dioxide bubble in water for various liquid heights. A constant initial bubble size was used, and little difference is noticeable from this plot. However, due to an increased concentration driving force at deeper sparger depths, the bubble has slightly higher mass transfer rates, and a slightly smaller diameter at any time relative to a shallower sparger height.

Weiner presents a correlation based on liquid physical properties which predicts the critical Reynolds number, Re_c, at which mass transfer description changes from the transition equation to Higbie's equation. The critical Reynolds number is given by:

$$Re_c = 4.02 \left[\frac{\gamma^3}{g\ \rho_L{}^3 \nu^4}\right]^{0.214} \tag{38}$$

where γ is liquid surface tension, and ν is the liquid kinematic viscosity. This Reynolds number is also the approximate value at which the drag coefficient deviates from the coefficient predicted for a sphere[21]. This correlation is strictly a function of liquid physical properties; accordingly, the Reynolds number is constant for any gas-liquid system. Weiner plots the Frossling, the transition, and the Higbie equations on log-log paper; all three equations plot as straight lines Figure (12). Hamerton and Garner's transition equation will yield straight lines having different slopes when different Schmidt numbers, Sc, are used in the various gas-water systems. When the slope of the transition equation changes, the intersection can be calculated knowing the critical Reynolds, number, Re_c, and the slope of the transition equation. Mass transfer correlations based on Reynolds number can then be calculated for a variety of gas-water systems. This allows systems such as air-water and oxygen-water systems to be modeled.

Figure 11

LOG (BUBBLE VOLUME) VERSUS TIME FOR VARIOUS LIQUID HEIGHTS AND A CONSTANT INITIAL DIAMETER

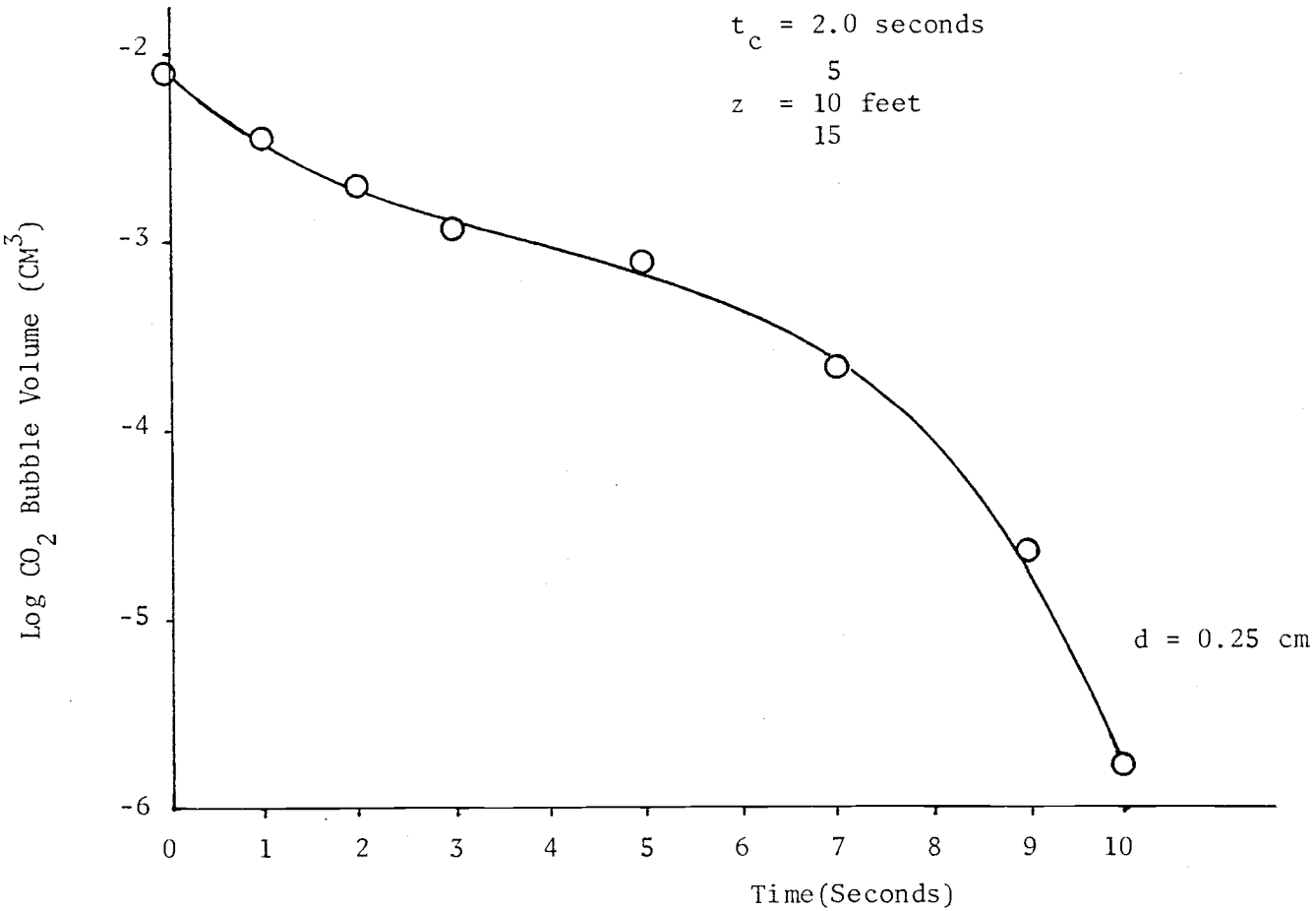

Figure 12

MASS TRANSFER CORRELATIONS: LOG (Sh) VERSUS LOG (Re)

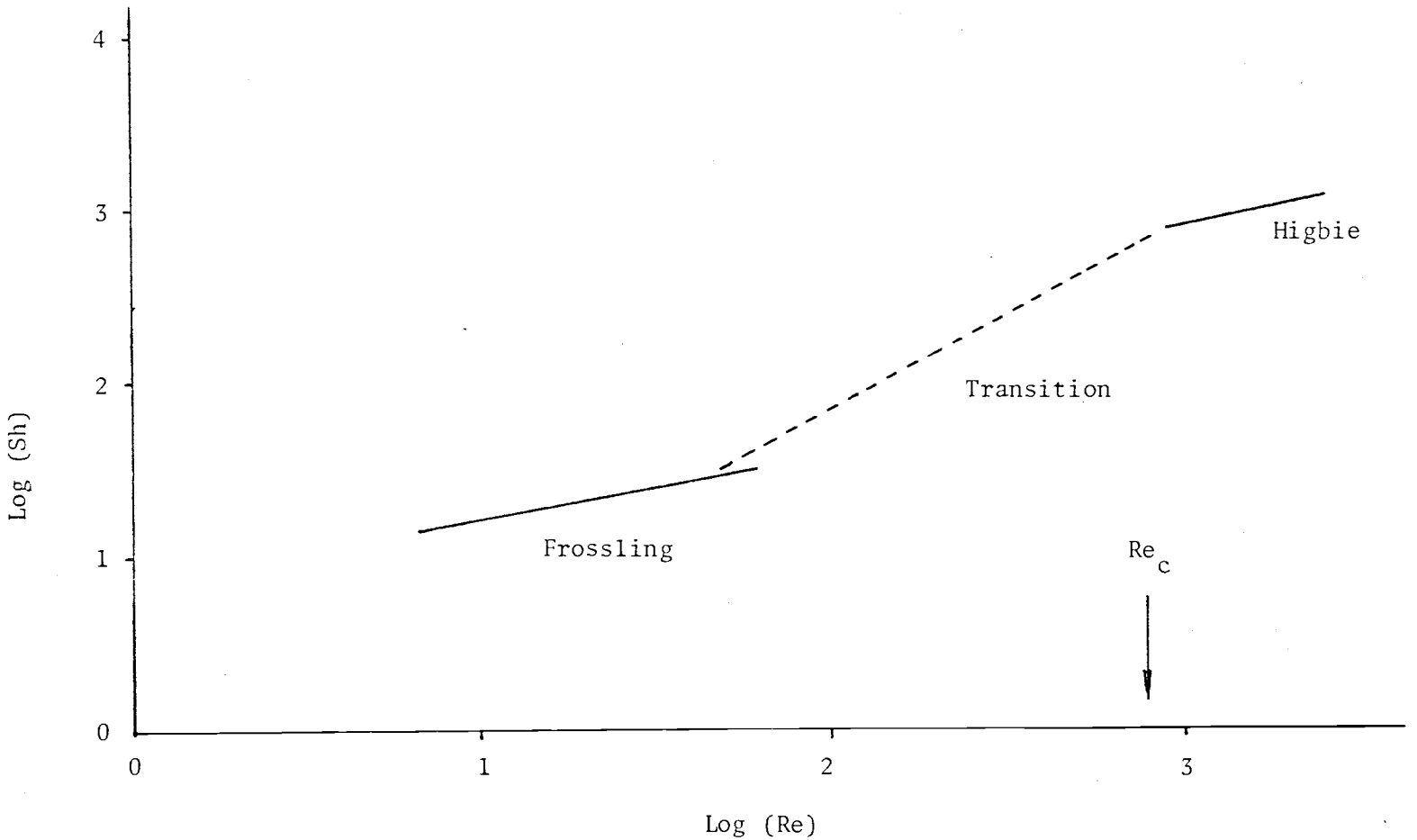

Pure oxygen and air are modeled by the introduction of the appropriate physical constants: Henry's law constant, Schmidt number, the gas molecular weight and the mass diffusivity. Program REST will model pure and two component gases. It treats two component gases as having one soluble and one insoluble component. Air is modeled as initially containing 21% oxygen with nitrogen being considered as insoluble.

Figure 13 plots a pure oxygen bubble's diameter versus time for an initial bubble diameter of 0.25 cm and liquid height of 6 feet. After 20 seconds, the bubble volume is observed in Figure 13 to be increasing with time, whereas the volume of a carbon dioxide bubble of an identical initial diameter always decreases with time. This demonstrates the opposing effects of mass transfer and decreasing hydrostatic head. Since the solubility of oxygen is approximately twenty-five times lower than the solubility of carbon dioxide a lower mass transfer rate for oxygen results. At these lower rates, the hydrostatic head decrease becomes more apparent and causes the bubble to expand.

Figure 14 plots the moles present of a pure oxygen bubble versus time, at various liquid heights. The initial bubble diameter was constant at 0.25 cm and t_c was equal to 2.0 seconds. For this case, the overall oxygen transfer was proportional to the ascent time or to the liquid height. This is a result of a relatively constant bubble diameter, surface area, and convective mass transfer coefficient. The majority of oxygen remains in the bubble, and is lost when the bubble burst at the surface.

Figure 16 plots the moles of oxygen present in an air bubble versus time at various liquid heights. The initial bubble diameter was constant at a diameter equal to 0.25 cm and t_c equal to 2.0 seconds. Overall oxygen transfer is again roughly proportional to the time of bubble ascent, and the majority of oxygen remains in the bubble prior to bursting at the liquid surface.

Figure 17 plots the moles of nitrogen present in a bubble of air versus time at various liquid heights. The initial bubble diameter is 0.25 cm and critical time constant is 2.0 seconds. Overall nitrogen transfer is roughly proportional to bubble ascent time, but the percentage of nitrogen transferred is only half that of oxygen. This is related to the solubility of nitrogen, which is roughly one half the solubility of oxygen.

In aeration, the desired parameter of interest for a constant sparger or liquid height, is the percent of oxygen transferred during the bubble ascent. For example, it may be desired to transfer 95 percent of the initial 0_2 present during the ascent. This requires an evaluation of what the initial diameter of the bubble should be. The percent oxygen transferred becomes the boundary condition of differential equation (1) and solution to this boundary value problem must be solved by guessing an initial bubble diameter and checking the total mass transfer against the desired value of percent oxygen transferred. This method of trial and error is called a "shooting problem." [1]

Figure 18 plots the percent oxygen transferred of air bubbles in water versus initial bubble diameter. Various initial bubble diameters were used to determine the percent oxygen transferred for a liquid height of 15 feet and t_c equal to 2.0 seconds.

Figure 15 plots the percent oxygen transferred of pure oxygen bubbles in water versus initial bubble diameter. Various initial bubble diameters were used to determine the percent oxygen transferred for a liquid height of 15 feet and t_c equal to 2.0 seconds.

Figures 15 and 18 both show the significance of initial bubble diameter upon the percent of oxygen transferred. As the initial bubble diameter decreases, a greater percentage of oxygen transfer is realized until virtually all of the oxygen has been transferred. The significance of the bubble's surface area to volume ratio is observed since the percent of oxygen transfer increases dramatically as the initial bubble diameter decreases.

Figure 13

OXYGEN BUBBLE DIAMETER VERSUS TIME

$z = 6.0$ feet

$t_c = 2.0$ seconds

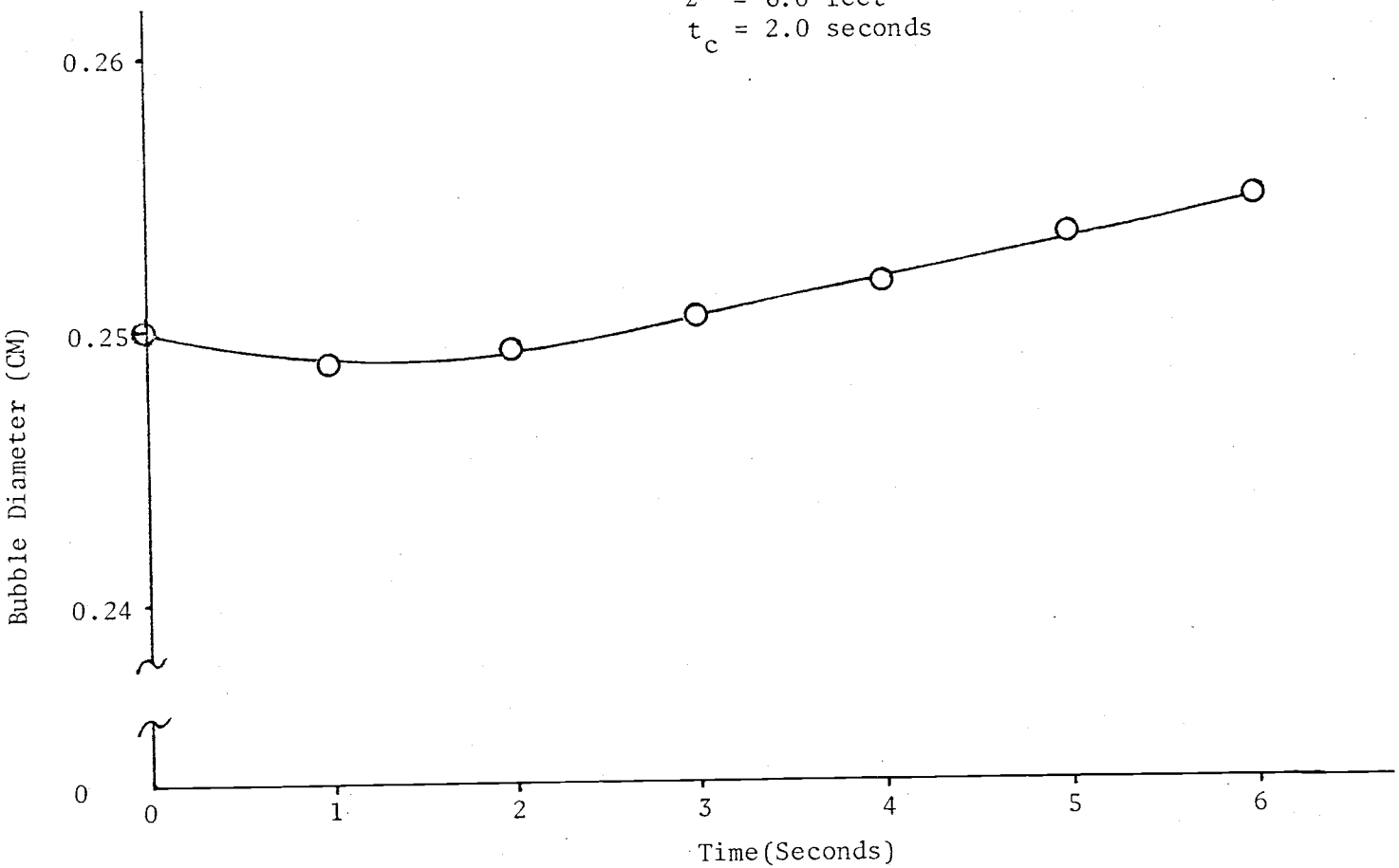

Figure 14

OXYGEN IN BUBBLES VERSUS TIME FOR VARIOUS LIQUID HEIGHTS
PURE OXYGEN

t_c = 2.0 seconds
d = 0.25 cm

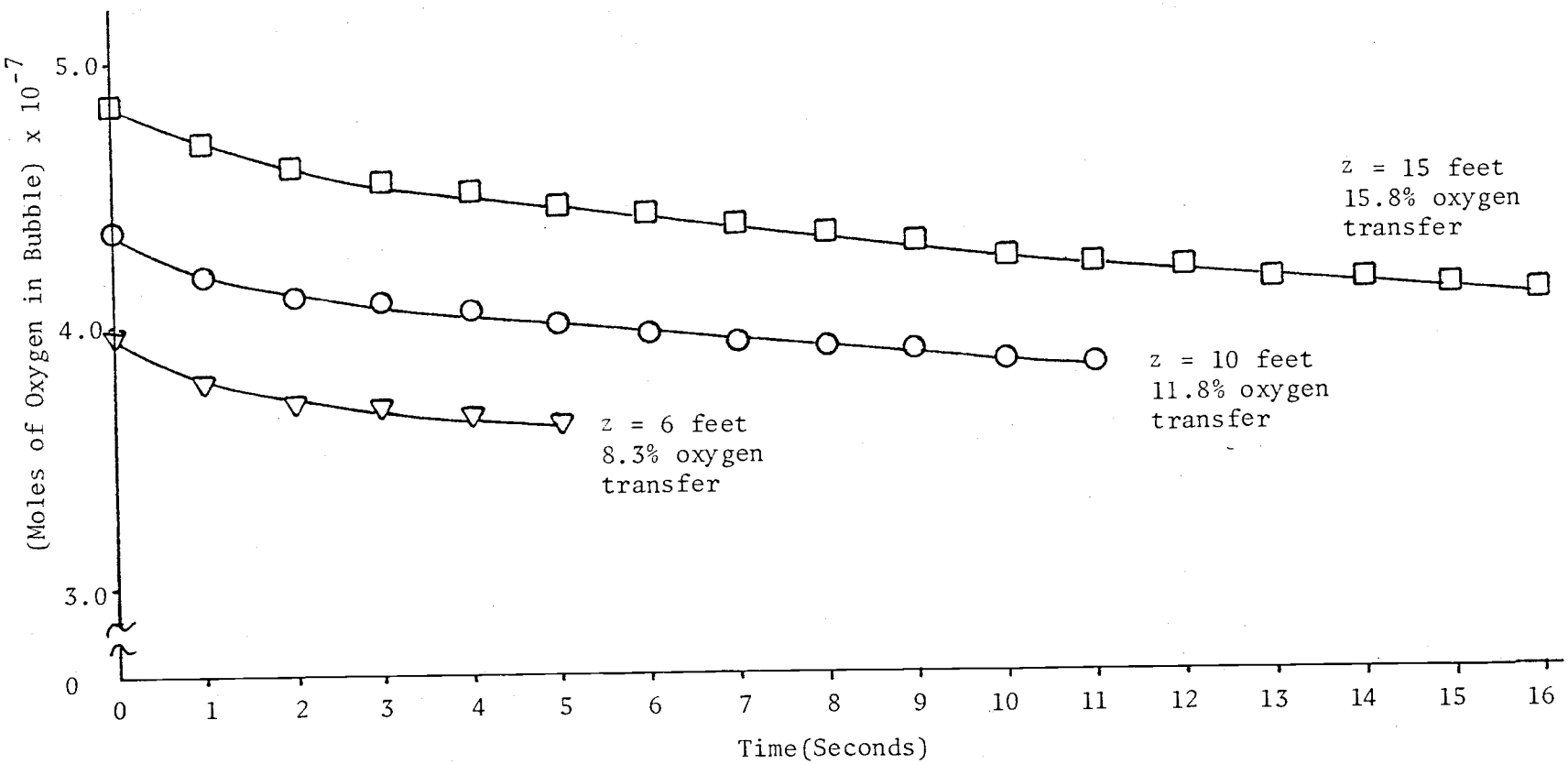

Figure 15
PERCENT OXYGEN TRANSFERRED VERSUS INITIAL BUBBLE DIAMETER
PURE OXYGEN

t_c = 2.0 seconds

z = 15 feet

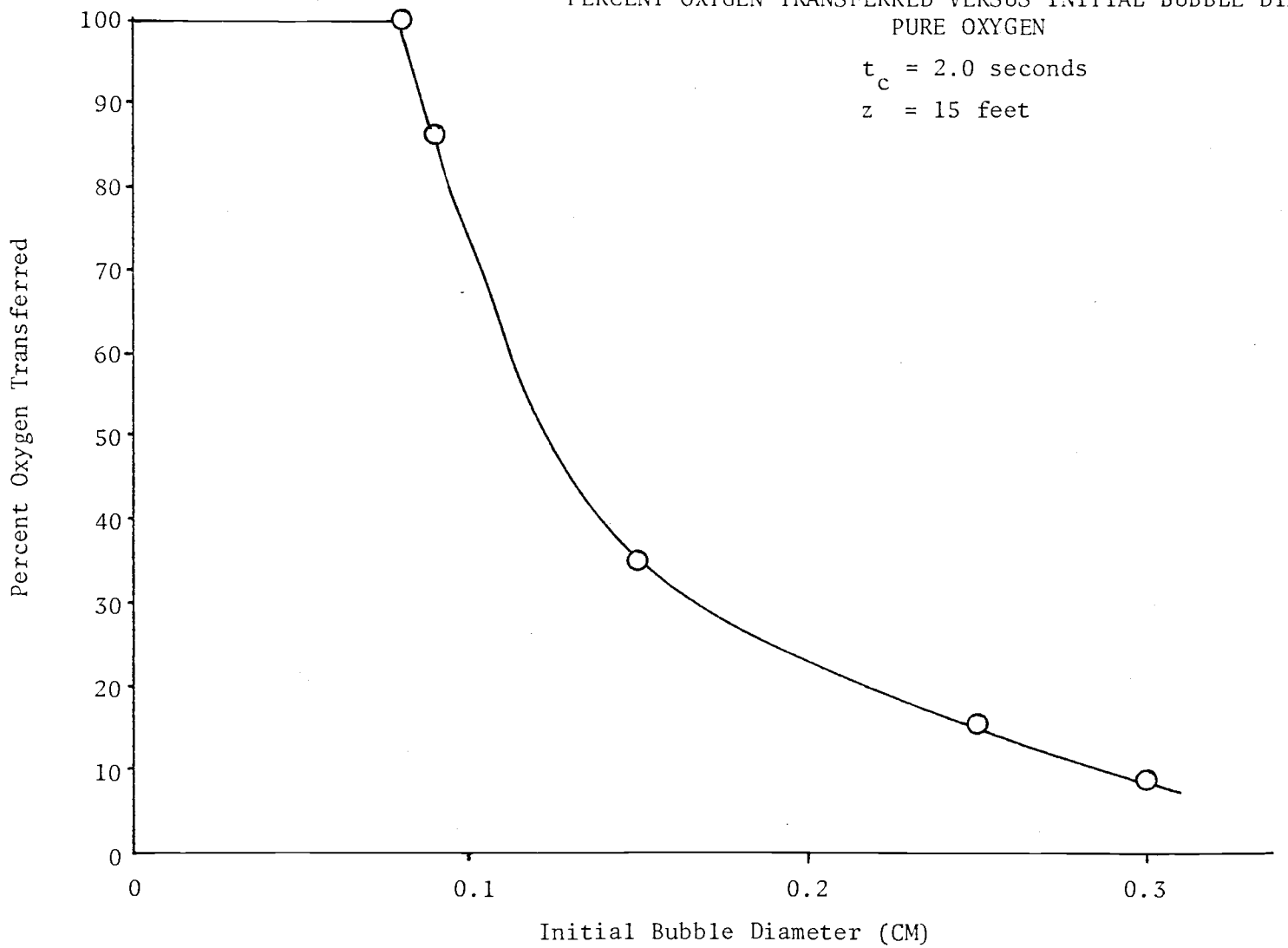

Figure 16

MOLES OF OXYGEN VERSUS TIME FOR VARIOUS LIQUID HEIGHTS
AIR (21% OXYGEN + INSOLUBLE)

t_c = 2.0 seconds
d = 0.25 cm

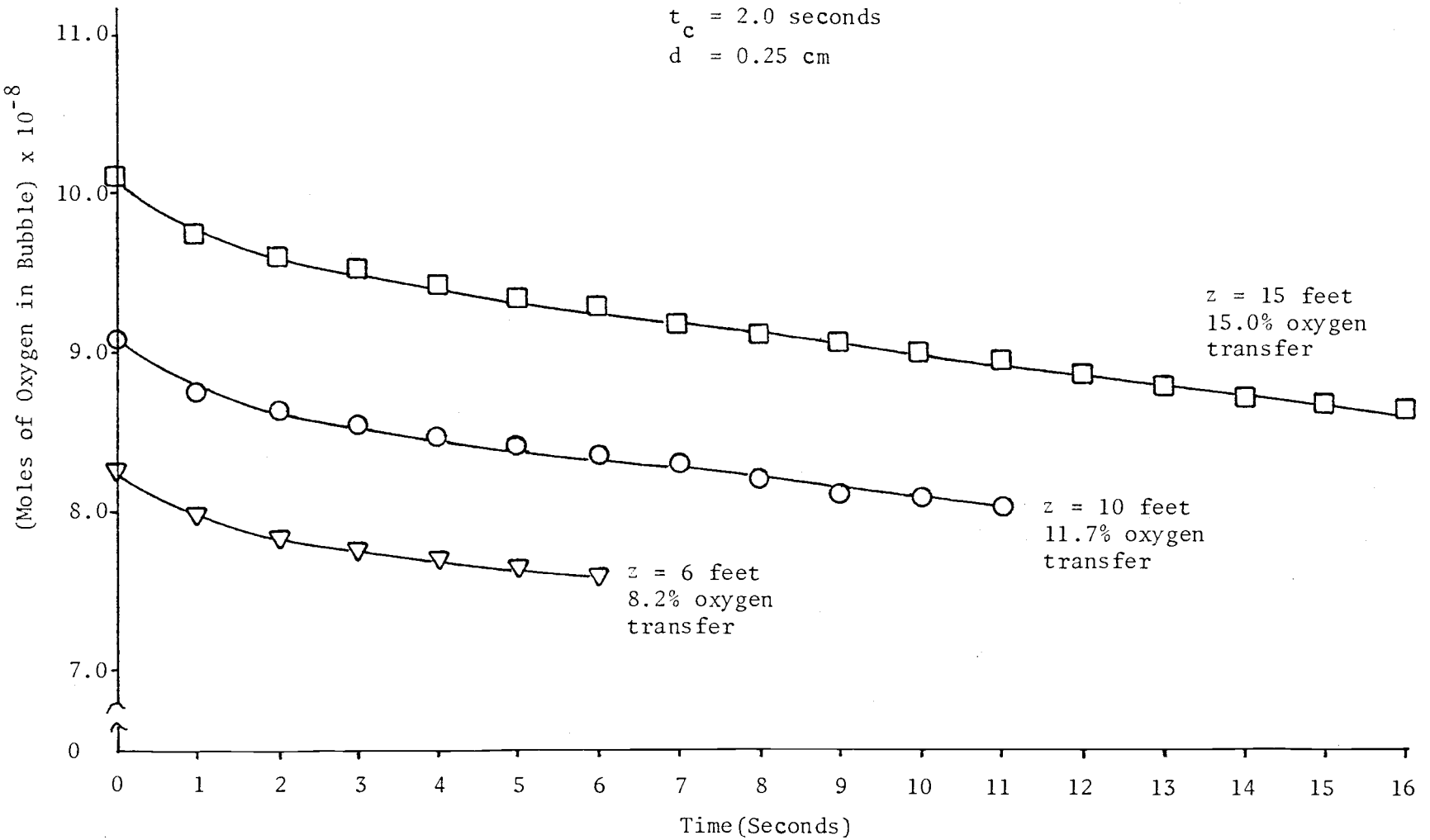

Figure 17

MOLES OF NITROGEN VERSUS TIME FOR VARIOUS LIQUID HEIGHTS
79% N_2 + INSOLUBLE FRACTION
t_c = 2.0 seconds
d = 0.25 cm

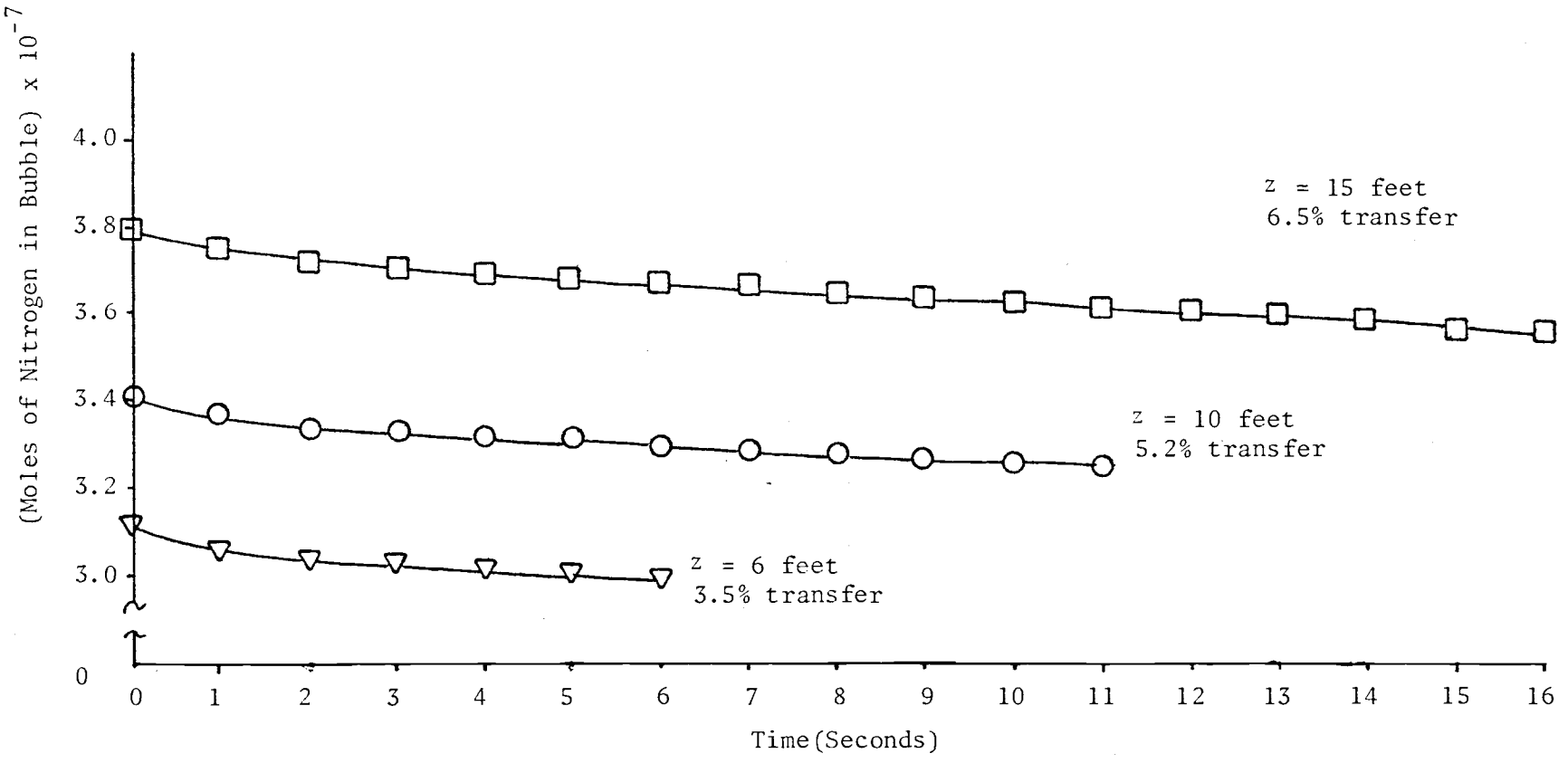

Figure 18

PERCENT OXYGEN TRANSFER IN AIR VERSUS INITIAL BUBBLE DIAMETER
21% O_2 + INSOLUBLE FRACTION
t_c = 2.0 seconds
z = 15 feet

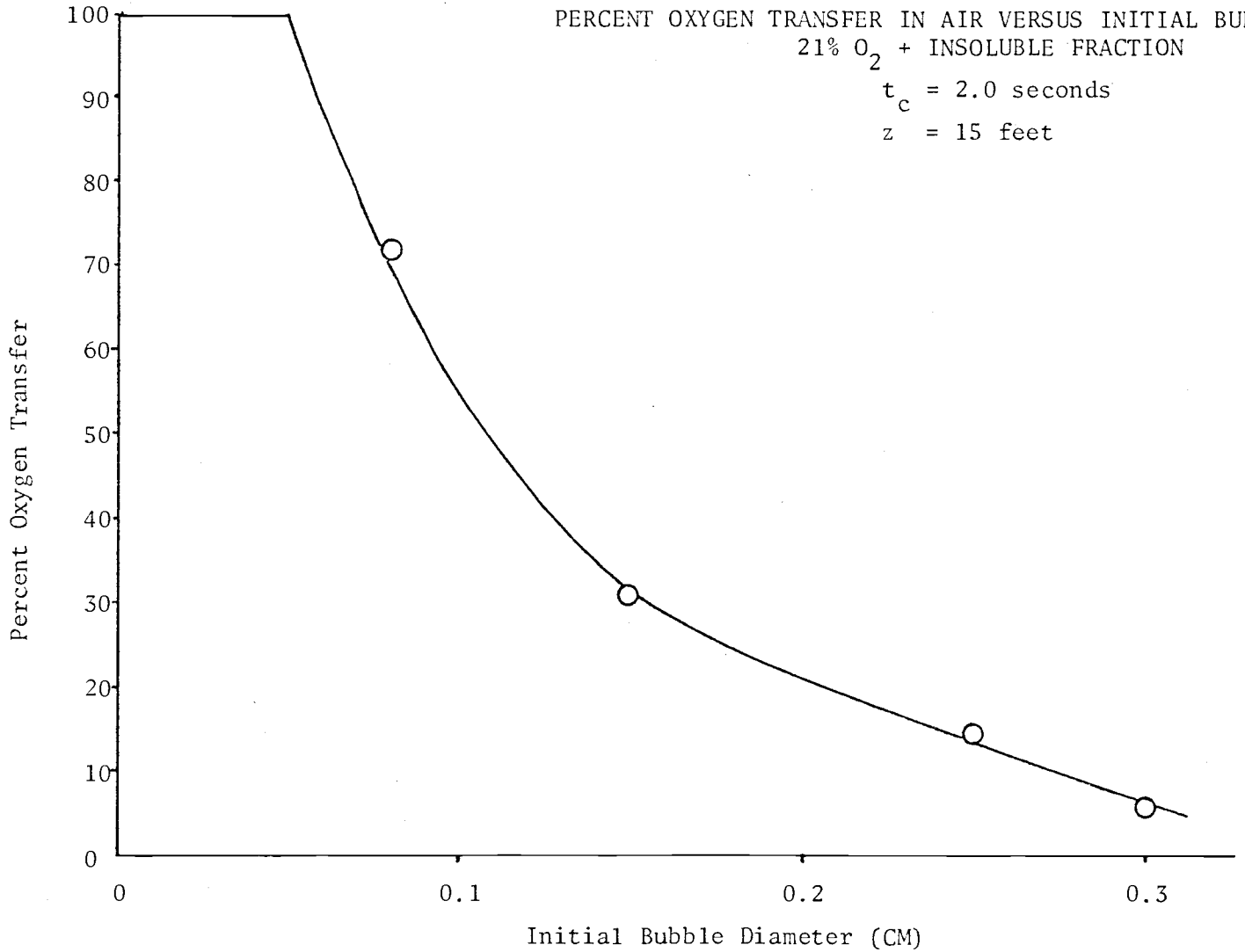

VI. CONCLUSION

A model which requires a critical time aging correlation has been developed and this model adequately describes mass transfer from single rising gas bubbles. The initial bubble diameter has a significant role in the overall mass transfer of a single bubble.

Future work should include provisions for multicomponent diffusion, and extension of the critical time concept to include bubble swarms, and mass transfer during bubble formation.

1. Carnahan, B., Luther, H.A., Wilkes, J.O., "The Approximation of the Solution of Ordinary Differential Equations," Applied Numerical Methods, 1st ed., John Wiley and Sons, New York, 1969.

2. Datta, R.L., Napier, D.H., Newitt, D.M., "The Properties and Behavior of Gas Bubbles Formed at a Circular Orifice," Transactions, Institution of Chemical Engineers, London, Vol. 28, 1950, pp. 14-26.

3. Deindoerfer, F.H., Humphrey, A.E., "Mass Transfer from Individual Gas Bubbles," Industrial and Engineering Chemistry, Vol. 53, No. 9, Sept. 1961, pp. 755-759.

4. Eckenfelder, W.W., Jr., "Absorption of Oxygen from Air Bubbles in Water," Proceedings Journal of the Sanitary Engineering Division, ASCE, Vol. 85, n SA4, Paper n 2090, July 1959, pp. 89-99.

5. Franks, R.G.E., "Numerical Solution of Differential Equations," Modeling and Simulation in Chemical Engineering, 1st ed., John Wiley and Sons, New York, New York, 1972, pp. 49-50.

6. Garbarini, G.R., Tien, C., "Mass Transfer from Single Gas Bubble - A Comparative Study on Experimental Methods," The Canadian Journal of Chemical Engineering, Vol. 47, Canada, Feb. 1969, pp. 35-41.

7. Griffith, R.M., "Mass Transfer from Drops and Bubbles," Chemical Engineering Science, Vol. 12, June 1960, pp. 198-213.

8. Hamerton, D., Garner, F.H., "Gas Absorption from Single Bubbles," Transactions Institution of Chemical Engineers, (British), Vol. 32, S18, 1954.

9. Higbie, R., "The Rate of Absorption of a Pure Gas into a Still Liquid During Short Periods of Exposure," Transactions, American Institute of Chemical Engineers, Vol. 31, No. 1, 1935, pp. 365-389.

10. Hougen, O., Watson, K., Ragatz, R.A., "Solubility and Crystallization," Chemical Process Principles, 2nd ed., John Wiley and Sons, New York, New York, 1965, pp. 181-183.

11. Houghton, G., McLean, A.M., Richtie, P.D., "Compressibility, Fugacity and Water Solubility of Carbon Dioxide in the Region 0-36 atm, and 0-100°C," Chemical Engineering Science, Vol. 6, Nov. 1957, pp. 132-137.

12. King, H.R., "Mechanics of Oxygen Absorption in Spiral Flow Aeration Tanks. I. Derivation of Formulas," Sew. Ind. Wastes, Vol. 27, 1955, p. 894.

13. Koide, K., Orito, Y., Hara, Y., "Mass Transfer from Single Bubbles in Newtonian Liquids," Chemical Engineering Science, Vol. 29, Feb. 1974, pp. 417-425.

14. Leonard, J.H., Houghton, G., "Mass Transfer and Velocity of Rise Phenomena for Single Bubbles," Chemical Engineering Science, Vol. 18, Feb. 1963, pp. 133-142.

15. Parkinson, W.J., DeNevers, N., "Partial Molal Volume of Carbon Dioxide in Water Solutions," Industrial and Engineering Chemistry, Fundamentals, Vol. 8, No. 4, Nov. 1969, p. 712.

16. Perry, R.H., Chilton, C.H., ed., "Transport Properties," Chemical Engineers Handbook, 5th ed., McGraw-Hill, New York, New York, 1973, pp. 3-224, 3-225.

17. Rosenbaum, E.J., "Liquids," Physical Chemistry, 1st ed., Meredith Corp., New York, New York, 1974, pp. 503-506.

18. Skelland, A.H.P., "Analogies Between Momentum and Mass Transfer," Diffusional Mass Transfer, 1st ed., John Wiley and Sons, New York, New York, 1970, pp. 273-277.

19. Speece, R.E., "The Case of Pure Oxygen in River and Impoundment Aeration," presented at the 24th Purdue Industrial Waste Conference, May 8, 1969.

20. Weast, R., ed., Handbook of Chemistry and Physics, 49th ed., The Chemical Rubber Co., Cleveland, Ohio, 1968-1969, pg. F30.

21. Weiner, A., Churchill, S.W., "Mass Transfer from Rising Bubbles," presented at the American Institute of Chemical Engineers meeting, March 16-20, 1975, held at Houston, Texas.

22. Welty, J.R., Wicks, C.E., Wilson, R.E., "Viscous Flow," Fundamentals of Momentum, Heat and Mass Transfer, 1st ed., John Wiley and Sons, New York, New York, 1969, pp. 156-160.

VIII. APPENDICES

APPENDIX A

Notation Used

			Unit	Dimensions
a	-	area through which mass transfer occurs	cm^2	L^2
C_{AS}	-	concentration of A in equilibrium with A in gas bubble	$mole/cm^3$	M/L^3
$C_{A\infty}$	-	concentration of A in bulk liquid	$mole/cm^3$	M/L^3
C_D	-	drag coefficient	dimensionless	
d	-	bubble diameter	cm	L
D_{AB}	-	diffusivity of A in B	cm^2/sec	L^2/t
e	-	truncation error		
f	-	function of		
g	-	gravitational constant	cm/sec^2	L/t^2
gr	-	grams	gr	M
Gr	-	Grashof number	$\frac{d^3\rho_L g\Delta\rho_L}{\mu^2}$	dimen-sionless
h	-	integration step size		
H	-	Henry's law constant	mole frac-tion/ATM	Lt^2/M
K_L	-	convective mass transfer coefficient	cm/sec	L/t
n	-	moles	moles	M
P	-	bubble internal pressure	ATM	M/Lt^2
P_{ATM}	-	atmospheric pressure	ATM	M/Lt^2
P_i	-	partial pressure of component i	ATM	M/Lt^2

R	-	ideal gas constant	$\frac{\text{ATM-cm}^3}{\text{g-mole-}^\circ\text{K}}$	
r	-	bubble radius	cm	L
Re	-	Reynolds number	$\frac{dV_o}{\nu}$	dimen-sionless
Sc	-	Schmidt number	$\frac{\nu}{D_{AB}}$	dimen-sionless
Sh	-	Sherwood number	$\frac{K_L d}{D_{AB}}$	dimen-sionless
t	-	time	sec	t
T	-	absolute temperature	°K	T
t_c	-	critical time	sec	t
V	-	bubble volume	cm^3	L^3
V_o	-	bubble rise velocity	cm/sec	L/t
x	-	mole fraction	dimensionless	
X	-	independent variable		
Y	-	dependent variable		
z	-	bubble position	cm(ft)	L

Greek Symbols

ρ	-	average density of static head	gr/cm^3	M/L^3
ρ_L	-	liquid density	gr/cm^3	M/L^3
ρ_g	-	bubble density	gr/cm^3	M/L^3
γ	-	surface tension	dynes/cm	M/t^2
ν	-	kinematic viscosity	cm^2/sec	L^2/t
μ	-	viscosity	gr/cm-sec	M/Lt
Δ	-	difference		
$\bar{\alpha}$	-	correlation factor	dimensionless	

APPENDIX B

Surface Tension Effects on a Bubble's Internal Pressure

For a spherical bubble, the internal pressure is [17]:

$$P = (P_{ATM} + \rho_L gz) + \frac{2\gamma}{r}$$, where γ is surface tension r is the bubble radius

or

$$\Delta P = \frac{2\gamma}{r}$$

The surface tension of water is:

γ = 71.97 dynes/cm @ 25°C [20]

Conversion from dynes/cm^2 x 9.869 x 10^{-7} = ATM

Letting r = 0.005 cm, d = 0.01 cm

$$\Delta P = \frac{2(71.97)}{5 \times 10^{-3}} = 2.88 \times 10^4 \text{ dynes/cm}^2$$

$$\Delta P = 28.4 \times 10^{-3} \text{ ATM}$$

$$\Delta P = 0.0284 \text{ ATM}$$

This ΔP will be negligible compared to the total hydrostatic head, where total head is: 1 - 1.4 ATM.

APPENDIX C

Bubble Force Balance

For an object where total drag is due to pressure as well as frictional effects [22].

$$\frac{F}{A_p} = C_D \frac{\rho_L V_\infty^2}{2} \qquad (A1)$$

A_p - maximum projected area $= \frac{\pi d^2}{4}$

F - total buoyant force $= (\rho_L - \rho_g)\, g \times$ bubble volume

$$= (\rho_L - \rho_g)\, g \frac{\pi d^3}{6}$$

Substituting into the left hand side of A1:

$$\frac{(\rho_L - \rho_g)\pi g\, d^3/6}{\pi d^2/4} = C_D \rho_L \frac{V_\infty^2}{2}$$

$$\frac{(\rho_L - \rho_g) g\, d\, 4}{6} = C_D \rho_L \frac{V_\infty^2}{2}$$

$$\frac{4d}{3} \frac{(\rho_L - \rho_g) g}{C_D \rho_L} = V_\infty^2$$

$$\left[\frac{4d(\rho_L - \rho_g) g}{3\, d\, C_D \rho_L}\right]^{1/2} = V_\infty \qquad (10)$$

APPENDIX D

Experimental Correlations of Forced Convection Mass Transfer from Single Spheres [18]

Table 1

Equation	Range of Variables	Reference
$Sh = 2 + 0.55\ Re^{1/2}Sc^{1/3}$	$2 < Re < 800$	Frossling (1938, 1940)
	$0.6 < Sc < 2.7$	Maxwell & Storrow (1957)
$Sh = 2 + 0.6\ Re^{1/2}Sc^{1/3}$	$2 < Re < 200$	Ranz & Marshall (1952)
	$0.6 < Sc < 2.5$	
$Sh = 2 + 0.54\ Re^{1/2}Sc^{1/3}$	$50 < Re < 350$	Hsu, Sato, & Sage (1954)
	$Sc = 1$	
$Sh = 2 + 0.95\ Re^{1/2}Sc^{1/3}$	$100 < Re < 700$	Garner & Suckling (1958)
	$1200 < Sc < 1525$	
$Sh = 2 + 0.575\ Re^{1/2}Sc^{0.35}$	$1 < Re$	Griffith (1960)
	$1 < Sc$	
$Sh = 2 + 0.79\ Re^{1/2}Sc^{1/3}$	$20 < Re < 2000$	Rowe, Claxton, & Lewis (1965)

APPENDIX E

Penetration Model for a Bubble

$$K_L = 2 \left[\frac{D_{AB}}{\pi t_{exp}} \right]^{1/2}$$ Higbie Penetration Model [9]

For a bubble $t_{exp} \cong$ bubble diameter/ bubble velocity

$$t_{exp} \cong d/V_o$$

$$K_L = 2 \left[\frac{D_{AB} V_o}{\pi d} \right]^{1/2}$$

This may be converted to the dimensionless Sherwood Number, Sh

$$\frac{K_L d}{D_{AB}} = 2 \left[\frac{D_{AB} V_o}{\pi d} \right]^{1/2} \cdot \frac{d}{D_{AB}}$$

$$= 2 \left[\frac{V_o d}{\pi D_{AB}} \right]^{1/2} \cdot \frac{\nu^{1/2}}{\nu^{1/2}}$$

$$= 2 \left[\frac{V_o d \nu}{\pi \nu D_{AB}} \right]^{1/2}$$

Since $\frac{V_o d}{\nu} = Re$ and $\frac{\nu}{D_{AB}} = Sc$,

$$Sh = 2 \left(\frac{1}{\pi} ReSc \right)^{1/2}$$

$$Sh = 1.13(ReSc)^{1/2} \qquad (14)$$

APPENDIX F

Regula-Falsi Technique

This method is used to solve for the root of an equation:

ie. $f(X) = 0$

Solve for X.

For the terminal velocity of a bubble, a function may be defined as:

$$V_0 = \left[\frac{4d(\rho_L-\rho_g)g}{3C_D\,\rho_L}\right]^{1/2} \qquad (10)$$

Trial and error involves guessing a value of V_0, determine C_D, the drag coefficient and solving for a subsequent V_0. If the guessed V_0 is equal to the calculated V_0, then that V_0 is correct.

Defining:

$$f(V_0) = \left[\frac{4d(\rho_L-\rho_g)g}{3C_D\,\rho_L}\right]^{1/2} - V_0 \text{ (assumed)} \qquad (A2)$$

$f(V_0) = 0$, when the correct value of V_0 is inserted.

Two values of V_L and V_r are set such that the

Sign $f(V_L) \neq$ Sign $f(V_r)$

or Sign $f(V_L) < 0$

Sign $f(V_r) > 0$

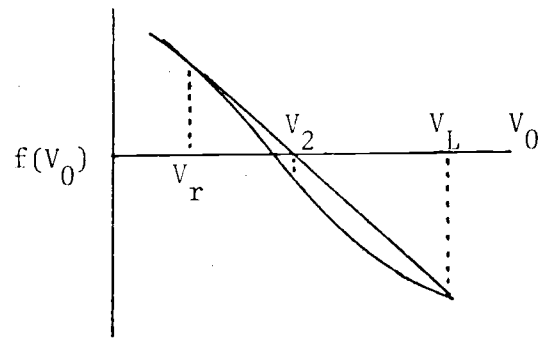

Two similiar triangles are formed, and the points $[V_L, f(V_L)]$,

$[V_r, f(V_r)]$ forming a straight line, with $f(V_2) = 0$. The straight line equation for $[V_L, f(V_L)]$, $[V_2, f(V_2)]$, $[V_r, f(V_r)]$ is:

$$\frac{f(V_2) - f(V_L)}{V_2 - V_L} = \frac{f(V_r) - f(V_L)}{V_r - V_L} \tag{A3}$$

But $f(V_2) = 0$ for straight line.

Solving for V_2 at that point:

$$\frac{0 - f(V_L)}{V_2 - V_L} = \frac{f(V_r) - f(V_L)}{V_r - V_L}$$

$$-f(V_L)\left[\frac{V_r - V_L}{f(V_r) - f(V_L)}\right] = V_2 - V_L$$

$$\frac{-V_r f(V_L) + V_L f(V_L)}{f(V_r) - f(V_L)} + V_L = V_2$$

$$\frac{-V_r f(V_L) + V_L f(V_L) + V_L f(V_r) - V_L f(V_L)}{f(V_r) - f(V_L)} = V_2$$

$$\frac{V_L f(V_r) - V_r f(V_L)}{f(V_r) - f(V_L)} = V_2 \tag{A4}$$

Values for V_L and V_r are determined by comparing the desired bubble diameter to values of diameter established in SUBROUTINE END (D,VL,VR). Previous hand calculations show how bubble velocity varies with diameter. Using these hand calculations as a rough estimate, values of V_L and V_r are determined by picking bubble diameters, less than and greater than the desired bubble diameter from figure 2.

V_2 is calculated by the derived equation. From the velocity function value of V_2, logic is employed to reassign the value of V_2 as either V_L or V_r. The subsequent straight lines have V_0 intercepts closer to the correct value of V_0. This iteration is repeated until the velocity function is close to zero. See the flowsheet for Regula-Falsi on the following page.

REGULA-FALSI LOGIC

$$f(V_o) = 0 = \left[\frac{4dg\ (\rho_L - \rho_g)}{3\ C_D \rho_L}\right]^{1/2} - V_{o\ guess} \qquad (A2)$$

pick V_L such that $f(V_L) < 0$

pick V_r such that $f(V_r) > 0$

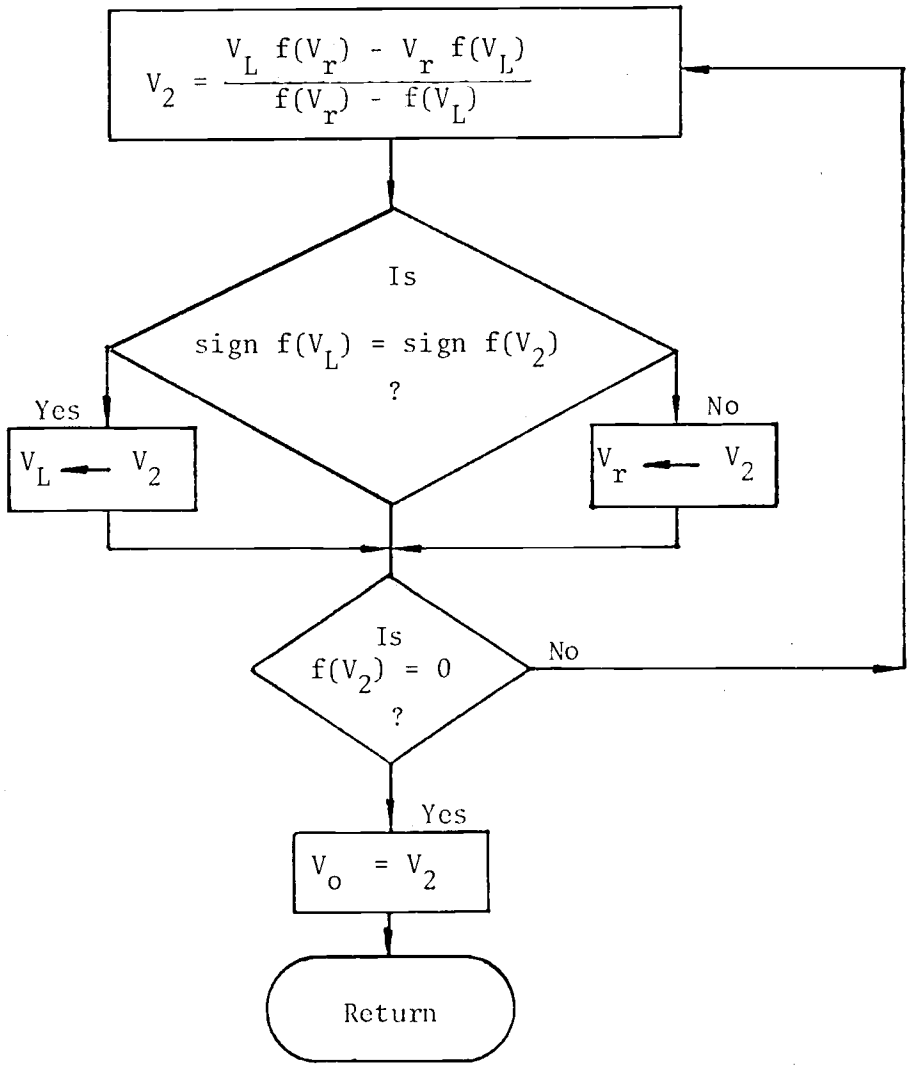

APPENDIX G

Error Criteria - Euler's Method [5]

For a function Y(X), the definition of Taylor's series expansion Y(X) about X_i is

$$Y(X_{i+1}) = Y(X_i) + hf(X_i, Y(X_i)) + \frac{h^2}{2!} f'(X_i, Y(X_i)) + \ldots$$

$$\ldots + \frac{h^n f^{(n-1)}}{n!} (X_i, Y(X_i)) + \frac{h^{n+1} f^{(n)}}{(n+1)!} (\xi, Y(\xi))$$

where ξ in the interval (X_{i+1}, X_i) (34)

Euler's approximation of $Y(X_{i+1})$ is:

$$Y(X_{i+1}) = Y(X_i) + hf(X_i, Y(X_i)) \quad (35b)$$

and the sum of the remaining terms of the Taylor's expansion of Y(X) represents the error of the approximation. Since Taylor's series converge fairly rapidly, the bulk of the error can be represented by the first term of the neglected series or:

$$e \cong \frac{h^2}{2!} f'(X_i, Y(X_i)) \quad (A5)$$

expanding the function f' by Taylor's series (approximation of a derivative):

$$f' = \frac{f(X_{i+1}, Y(X_{i+1})) - f(X_i, Y(X_i))}{h}$$

$$f' = \frac{f_{i+1} - f_i}{h} \quad (A6)$$

substitution of (A6) into (A5) yields:

$$e \simeq \frac{h^2}{2!} \left[\frac{f_{i+1} - f_i}{h}\right]$$

$$e \simeq \frac{h}{2!} \left[f_{i+1} - f_i\right] \qquad \text{(A7)}$$

The absolute truncation error, $|e|$, is simply the absolute value of the right hand side of equation (A7) and functional values of f_{i+1} and f_i are evaluated by program EULER and equation (A7) estimates the local truncation error. For equations (1) and (2) this truncation error is then compared to a desired accuracy, and the step size, h, is adjusted accordingly to maintain the desired accuracy.

APPENDIX H

Natural Convection Effects

Natural convection effects are negligible compared to forced convection if the expression holds: [18]

$$Re > 0.4\ Gr^{1/2}\ Sc^{-1/6} \qquad (A8)$$

where Gr is the Grashof number and:

$$Gr = \frac{d^3 \rho_L g \Delta\rho_L}{\mu^2}$$

At 25°C, the density of pure water is:

$$\rho_L = 0.9964\ gr/cm^3$$

and the density of carbon dioxide-water solution at a partial pressure of one-two ATM is: [15]

$$\rho_L = 0.997$$

or $\Delta\rho_L$ is equal to:

$$\Delta\rho_L = 0.997 - 0.9964 = 6.0 \times 10^{-4}\ gr/cm^3$$

The remaining physical constants are:

$$\mu = 8.93 \times 10^{-3}\ gr/cm - sec$$

$$g = 980.\ cm/sec^2$$

Solving for Gr yields:

$$Gr = \frac{d^3(0.9964)(980)(6 \times 10^{-4})}{(8.93 \times 10^{-3})^2} \qquad \frac{(cm^3)(gr/cm^3)(cm/sec^2)(gr/cm^3)}{(gr/cm - sec)^2}$$

or: $Gr = 7346\ d^3$

The approximate range of d is:

$$0.05 < d < 0.35 \text{ cm}$$

Checking the Gr number at the extremes of the range:

$d = 0.35$	$Sc = 432$	$d = 0.05$
$Gr = 7346\ (0.35)^3$		$Gr = 7346\ (0.05)^3$
$Gr = 315$		$Gr = 0.918$

A bubble rise velocity yields the corresponding Re:

$d = 0.35$	$d = 0.05$
$Re = 1112$	$Re = 19.75$

From the relationship of A8:

$1112 \overset{?}{>} 0.4(315)^{1/2}(432)^{-1/6}$	$19.75 \overset{?}{>} 0.4(0.918)^{1/2}(432)^{-1/6}$
$1112 > 2.57$	$19.75 > 0.139$

Then natural convection effects are negligible compared to forced convection.

APPENDIX I

Gas-Water Physical Properties

Gas-water diffusivities @ 25°C [16]

Carbon dioxide	1.96×10^{-5} cm^2/sec
@ 27°C	(1.987×10^{-5})* cm^2/sec
Oxygen	2.50×10^{-5} cm^2/sec
Nitrogen	1.90×10^{-5} cm^2/sec

Kinematic viscosity - water [22]

@ 25°C 8.668×10^{-3} cm^2/sec

@ 27°C (8.593×10^{-3})* cm^2/sec

Schmidt numbers	ν/D_{AB}	Sc	$Sc^{1/3}$
Carbon dioxide =	$\frac{8.593 \times 10^{-3} \text{ cm}^2/\text{sec}}{1.987 \times 10^{-5} \text{ cm}^2/\text{sec}}$	432*	7.559
Oxygen =	$\frac{8.668 \times 10^{-3} \text{ cm}^2/\text{sec}}{2.50 \times 10^{-5} \text{ cm}^2/\text{sec}}$	346	7.020
Nitrogen =	$\frac{8.668 \times 10^{-3} \text{ cm}^2/\text{sec}}{1.90 \times 10^{-5} \text{ cm}^2/\text{sec}}$	456	7.698

Henry's law constants:	25°C (mole frac/ATM)	Reference
Carbon dioxide	6.08×10^{-4}	[11]
Oxygen	2.30×10^{-5}	[10]
Nitrogen	1.14×10^{-5}	[10]

*These values were used in the computer model instead of the values listed @ 25°C.

```
      PROGRAM FLST
      COMMON PRESS
      REAL INERT
      DATA(TEMP=293.),(GAS=32.05),(E=0.001),(PI=3.14159),
     1(XMAX=0.001),(PI=3.14159)
      DIMENSION Y(10),F(10)
C
C     INITIAL VALUES
C
      X=0.
      H=TTYIN(4H H= )
      D=TTYIN(4H D= )
      Z=TTYIN(4H Z= )
      AGE=TTYIN(4HAGE=)
      PART=TTYIN(4HPART)
      Z0=Z
      VOL=PI*D**3/6.
      PRESS=(Z+34.)/34.
      AREA=PI*D**2
      Y(1)=Z/PI0
      Y(2)=VOL*PRESS/GAS/TEMP*PART
      INERT=VOL*PRESS/GAS/TEMP*(1.-PART)
      YA=Z
      WRITE(61,90)X,D,Z,VOL,Y(2)
   90 FORMAT(4X,'TIME',6X,'DIAMETER',7X,'HEIGHT ',4X,'VOLUME'
     1,5X,'MOLS',5X,'MOL FRAC',//3X,F7.4,2X,F9.5,3X,F10.4,2X,
     1E11.3,2X,E11.3)
C
C     CALCULATION OF F(J) FOR ALL EQNS (DIFF. EQNS)
C
   10 CALL FKN(2,X,Y,F,H,IFKN,E,1.0)
      IF(IFKN.EQ.2)GO TO 11
      V=PRESS(D)
      F(1)=-V
      F(2)=-COEF(V,D,X,AGE)*AREA*CONC(YA,PART)
      GO TO 10
   11 Z=Y(1)*PI0
      PRESS=(Z+34.)/34.
      VOL=(Y(2) + INERT)*GAS*TEMP/PRESS
      PART=Y(2)/(Y(2)+INERT)
      D=((6.*VOL)/PI)**0.33333
      AREA=PI*D**2
      YA=Z
      WRITE(61,91)X,D,Z,VOL,Y(2),PART
   91 FORMAT(3X,F7.4,2X,F9.5,3X,F10.4,2X,E11.3,2X,E11.3,F10.5)
      IF(Z-YMAX.GT.0.001)GO TO 10
      END
```

```
      FUNCTION CONV(VEL,D,X,ACE)
      DATA (SC=346.),(DIFF=2.5E-5)
      DATA (MU=8.593E-3)
      REAL MU
C
C     THIS FUNCTION CALCULATES MASS TRANSFER COEFF.
C     BASED UPON EITHER FROSSLING EQN OR TRANSITION EQN
C     AND USES A WEIGHT FACTOR BASED UPON THE CRITICAL
C     TIME CONSTANT
C
C     TRANSITION EQN
C
      SM=SC**.33333
      RE = VEL*D/MU
      IF(RE.LE.60.)GO TO 20
      SHERT = 0.11*SM*RE
C
C     FROSSLING EQN CALCULATION
C
      SHERF = 2. + 0.55*SM*SQRT(RE)
      IF(X.GT.ACE)GO TO 22
      CONV =((1.-X/ACE)*SHERT+X/ACE*SHERF)*DIFF/D
      RETURN
   22 CONV = SHERF*DIFF/D
      RETURN
   20 SHER=2. + 0.55*SM*SQRT(RE)
      CONV = SHER*DIFF/D
      RETURN
      END



      FUNCTION CONC(Z,PART)
      DATA (PROP=0.055278),(HENRY=2.3E-5)
C
C
C     TIS FUNCTION CALCULATES THE EQILIBRIUM CONC. OF
C     CO2 IN WATER FOR A GIVEN PRESSURE.  USES HENRYS
C     LAW AND CONC UNITS IN MOL/CM**3
C
      PRESS = (Z + 34.)/34.*PART
      FRAC = HENRY*PRESS/(1.-HENRY*PRESS)
      CONC = FRAC*PROP
      RETURN
      END
```

```
      FUNCTION RISE(D,VEL)
      REAL MOL,MW,MU
      COMMON PRESS
      DATA(GRAV=981.),(MW=32.),(MU=8.593E-3),(TEMP=298.)
     1,(GAS=82.05),(PI=3.14159),(ROL=.995)
      VOL=PI*D**3/6.
      MOL=PRESS*VOL/GAS/TEMP
      ROGAS=MOL*MW/VOL
C
C     THIS FUNCTION CALCULATES THE TERMINAL VELOCITY FUNCTION
C     IN THE FORM SUITABLE FOR THE REGULA FALSI TECHNIQUE
C     SOLVING THE SOLUTION OF AN EQUATION
C
      REN=D*VEL/MU
      PROP=4.*GRAV/(3.*ROL)
C
      RISE=SQRT(PROP*D*(ROL-ROGAS)/DRAG(REN))-VEL
      RETURN
      END



      FUNCTION DRAG(RA)
      DIMENSION RE(12),CD(12)
      DATA(RE=-0.301030,0.0,0.301030,0.698970,1.0,
     11.301030,1.698970,2.0,2.301030,2.698970,3.0,3.301030)
      DATA(CD=1.698970,1.342423,1.149219,0.851258,
     10.628389,0.484300,0.136721,0.0,-0.151811,-0.301030,
     1-0.371611,-0.406714)
C
C     CALCLATE DRAG COEFF. BY LINEAR INTERPLATION FO  OF DRAG VS
C     REYNOLDS NO. OF DATA FOR A SOLID SPHERE
C
      IF(RA.LT.0.5)GO TO 30
      RL=ALOG10(RA)
      DO 20 K=1,12
      IF(RL.LT.RE(K))GO TO 15
   20 CONTINUE
      IF(RA.GT.2000.)GO TO 25
   15 FRAC=(RL-RE(K-1))/(RE(K)-RE(K-1))
      DOG=CD(K-1)-FRAC*(CD(K-1)-CD(K))
      DRAG=10.**DOG
      RETURN
   30 DRAG=24./RA
      RETURN
   25 DRAG=0.392
      RETURN
      END
```

```
      SUBROUTINE END(D,VL,VR)
      DIMENSION V(10),DIA(10)
      DATA(V=0.0,.66,2.19,5.09,11.4,21.,29.,36.,41.,45.5)
      DATA(DIA=0.0,.01,.025,.05,.1,.2,.3,.4,.5,.6)
C
C     THIS FUNCTION CALCULATES AN INITIAL VELOCITY SUITABLE FOR
C     THE LIMITS OF THE REGULA FALSI TECHNIQUE
C
      IF(D.LE.0.025)GO TO 30
      DO 15 JI=3,10
      IF(D.LE.DIA(JI))GO TO 25
   15 CONTINUE
      WRITE(61,95)D
   95 FORMAT(10X,'DIAMETER OUTSIDE OF DATA RANGE  DIA=',F8.4)
      RETURN
   25 VL=V(JI+1)
      IF(DIA(JI)-D.GT.0.03)VL=V(JI)
      VR=V(JI-1)
      IF(D-DIA(JI-1).LT..02)VR=V(JI-2)
      RETURN
   30 VR=0.001
      VL=3.
      RETURN
      END
```

```
      FUNCTION REGULA(D)
      DATA(TOL=.00001)
C
C     THIS FUNCTION CALCULATES A BUBBLES TERMINAL VELOCITY
C     BY THE REGULA FALSI TECHNIQUE
C
      CALL END(D,VL,VR)
   16 VEL2=(VL*RISE(D,VR)-VR*RISE(D,VL))/(RISE(D,VR)-
     1RISE(D,VL))
C
      IF(RISE(D,VEL2).LT.0..AND.RISE(D,VL).LT.0..OR.
     1RISE(D,VEL2).GT.0..AND.RISE(D,VL).GT.0.)GO TO 10
      VR=VEL2
      GO TO 15
   10 VL=VEL2
   15 IF(ABS(RISE(D,VEL2)).LT.0.00001)GO TO20
      GO TO 16
   20 REGULA = VEL2
      RETURN
      END
```

H= .1
D= .285
Z= 4.92
AGE=2.
PART1.

TIME	DIAMETER	HEIGHT	VOLUME	MOLS	MOL FRAC
0	.28500	4.9200	1.212E-02	5.675E-07	
.1000	.27579	4.8232	1.098E-02	5.129E-07	1.00000
.3000	.25835	4.6339	9.029E-03	4.196E-07	1.00000
.7000	.22774	4.2723	6.184E-03	2.847E-07	1.00000
1.0000	.21119	4.0240	4.932E-03	2.256E-07	1.00000
1.5000	.19063	3.6314	3.627E-03	1.642E-07	1.00000
2.0000	.17896	3.2663	3.001E-03	1.345E-07	1.00000
3.0000	.16193	2.5742	2.223E-03	9.780E-08	1.00000
4.0000	.14430	1.9381	1.573E-03	6.801E-08	1.00000
5.0000	.12595	1.3612	1.046E-03	4.449E-08	1.00000
6.0000	.10664	.8469	6.349E-04	2.661E-08	1.00000
7.0000	.08613	.4067	3.345E-04	1.385E-08	1.00000
8.0000	.06375	.0515	1.356E-04	5.555E-09	1.00000
9.0000	.03558	-0.2153	2.358E-05	9.584E-10	1.00000

END OF FORTRAN EXECUTION

Best scan avilable. Original copy faded.

R= .1
D= .53
Z= 4.98
ACF=4.
RATIO.

TIME	DIAMETER	HEIGHT	VOLUME	MOLS	MOL FRAC
0	.53000	4.9800	7.795E-02	3.049E-06	
.1000	.51733	4.7688	7.249E-02	3.38?E-06	1.[illegible]
.3000	.49947	4.5098	6.853E-02	?.?97E-06	1.[illegible]
.7000	.44479	3.9784	4.60?E-02	2.105E-06	1.[illegible]
1.0000	.41479	3.5997	3.737E-02	1.69?E-06	1.[illegible]
1.5000	.36996	?.9941	2.651E-02	1.1??E-06	1.[illegible]
2.0000	.33476	2.4883	1.904E-02	?.607E-07	1.[illegible]
3.0000	.28168	1.3616	1.170E-02	4.977E-07	1.[illegible]
4.0000	.25?1	.4018	?.?88E-03	3.678E-07	1.[illegible]
5.0000	.24295	-?.4996	7.50?E-03	3.02?E-07	1.[illegible]

END OF FORTRAN EXECUTION

R= .1
D= .569
Z= 14.96
ACF=4.
PAR 1.

TIME	DIAMETER	HEIGHT	VOLUME	MOLS	VOL FRAC
0	.56900	14.9600	9.646E-02	5.681E-06	
.1000	.55579	14.8172	8.989E-02	5.279E-06	1.00000
.3000	.52991	14.5350	7.791E-02	4.549E-06	1.00000
.7000	.48848	13.9839	5.806E-02	3.351E-06	1.00000
1.0000	.44918	13.5904	4.745E-02	2.710E-06	1.00000
1.5000	.40231	12.9561	3.409E-02	1.926E-06	1.00000
2.0000	.36547	12.3615	2.556E-02	1.425E-06	1.00000
3.0000	.31651	11.2362	1.566E-02	8.530E-07	1.00000
4.0000	.28538	10.2154	1.217E-02	6.473E-07	1.00000
5.0000	.27158	9.8492	1.049E-02	5.456E-07	1.00000
6.0000	.25746	8.3134	8.937E-03	4.549E-07	1.00000
7.0000	.24303	7.4117	7.515E-03	3.724E-07	1.00000
8.0000	.22221	6.5456	6.223E-03	3.035E-07	1.00000
9.0000	.21299	5.7167	5.059E-03	2.417E-07	1.00000
10.0000	.19731	4.9269	4.022E-03	1.833E-07	1.00000
11.0000	.18112	4.1762	3.111E-03	1.429E-07	1.00000
12.0000	.16441	3.4790	2.327E-03	1.049E-07	1.00000
13.0000	.14714	2.8347	1.666E-03	7.391E-08	1.00000
14.0000	.12920	2.2462	1.129E-03	4.923E-08	1.00000
15.0000	.11038	1.7288	7.048E-04	3.026E-08	1.00000
16.0000	.09346	1.2670	3.675E-04	1.624E-08	1.00000
17.0000	.06698	.8939	1.718E-04	7.212E-09	1.00000
18.0000	.04361	.6065	4.343E-05	1.600E-09	1.00000